The Abdus Salam International Centre for Theoretical Physics

United Nations Educational, Scientific and Cultural Organization

IAEA International Atomic Energy Agency

CEI CENTRAL EUROPEAN INITIATIVE

2265-31

Advanced School on Understanding and Prediction of Earthquakes and other Extreme Events in Complex Systems

26 September - 8 October, 2011

Overview of Nuclear Techniques for Probing Earth's Interior and Earthquake Prediction
Part 1 - Part 2

Wolfango Plastino

National Institute of Nuclear Physics
Section of Roma Tre & Gran Sasso National Laboratory
Italy

Strada Costiera 11, 34151 Trieste, Italy - Tel.+39 040 2240 111; Fax +39 040 224 163 - sci_info@ictp.it

Overview of Nuclear Techniques for Probing Earth's Interior and Earthquake Prediction

Part 1 - Part 2

Wolfango Plastino

Department of Physics - University of Roma Tre
National Institute of Nuclear Physics - Section of Roma Tre and Gran Sasso National Laboratory

plastino@fis.uniroma3.it
wolfango.plastino@roma3.infn.it

ROMA TRE UNIVERSITÀ DEGLI STUDI

ERMES Environmental Radioactivity Monitoring for Earth Sciences

INFN Istituto Nazionale di Fisica Nucleare

Outline

- Overview: Nuclear Physics and Radioactivity
- Earth's Interior: a view from Solid Earth Physics to Nuclear Physics
- Nuclear Physics for probing Earth's Interior and Earthquake prediction

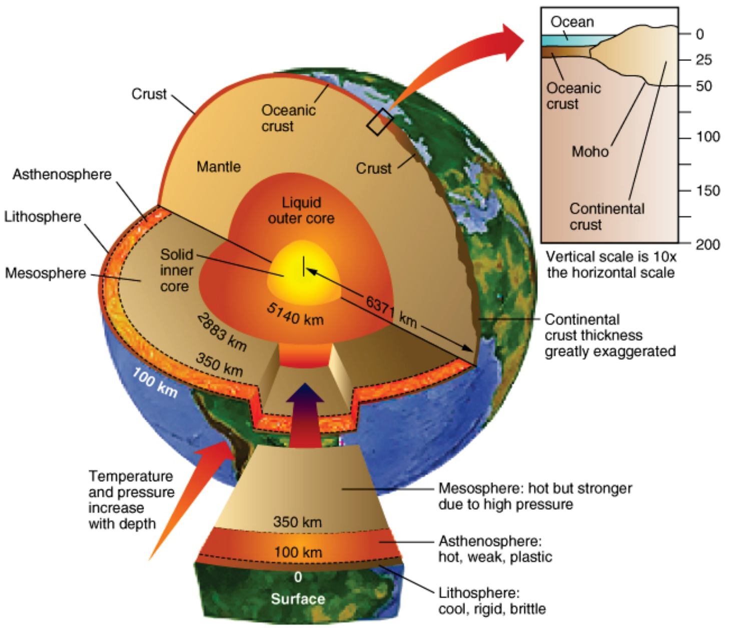

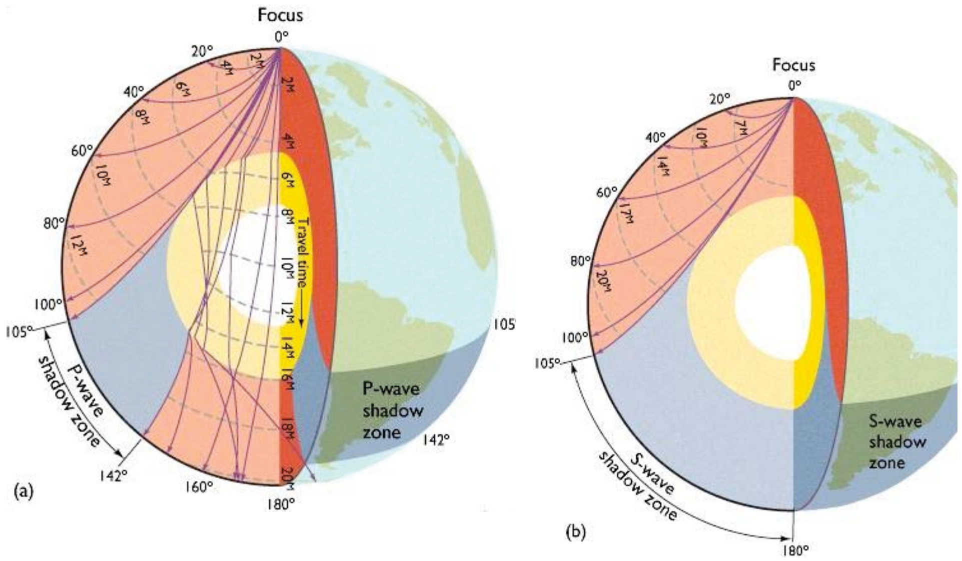

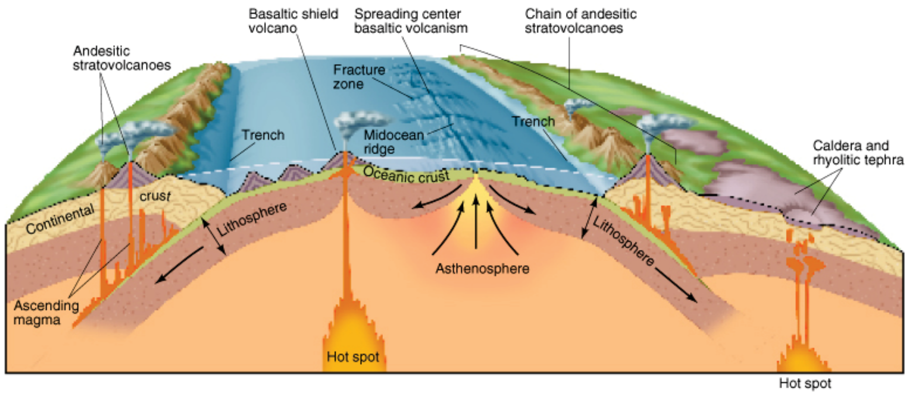

A Digital Age Map of the Ocean Floor

R. Dietmar Müller, Walter R. Roest, Jean-Yves Royer, Lisa M. Gahagan, and John G. Sclater

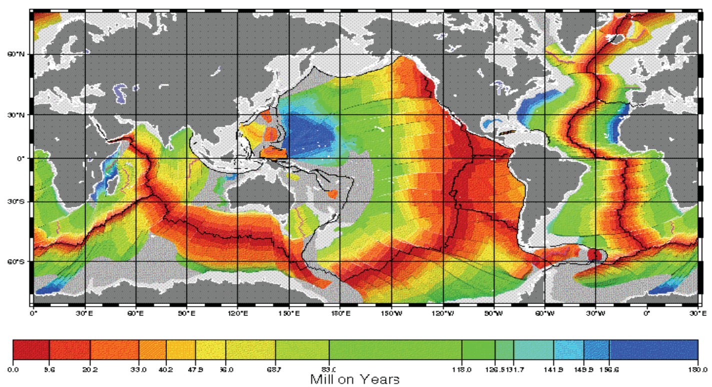

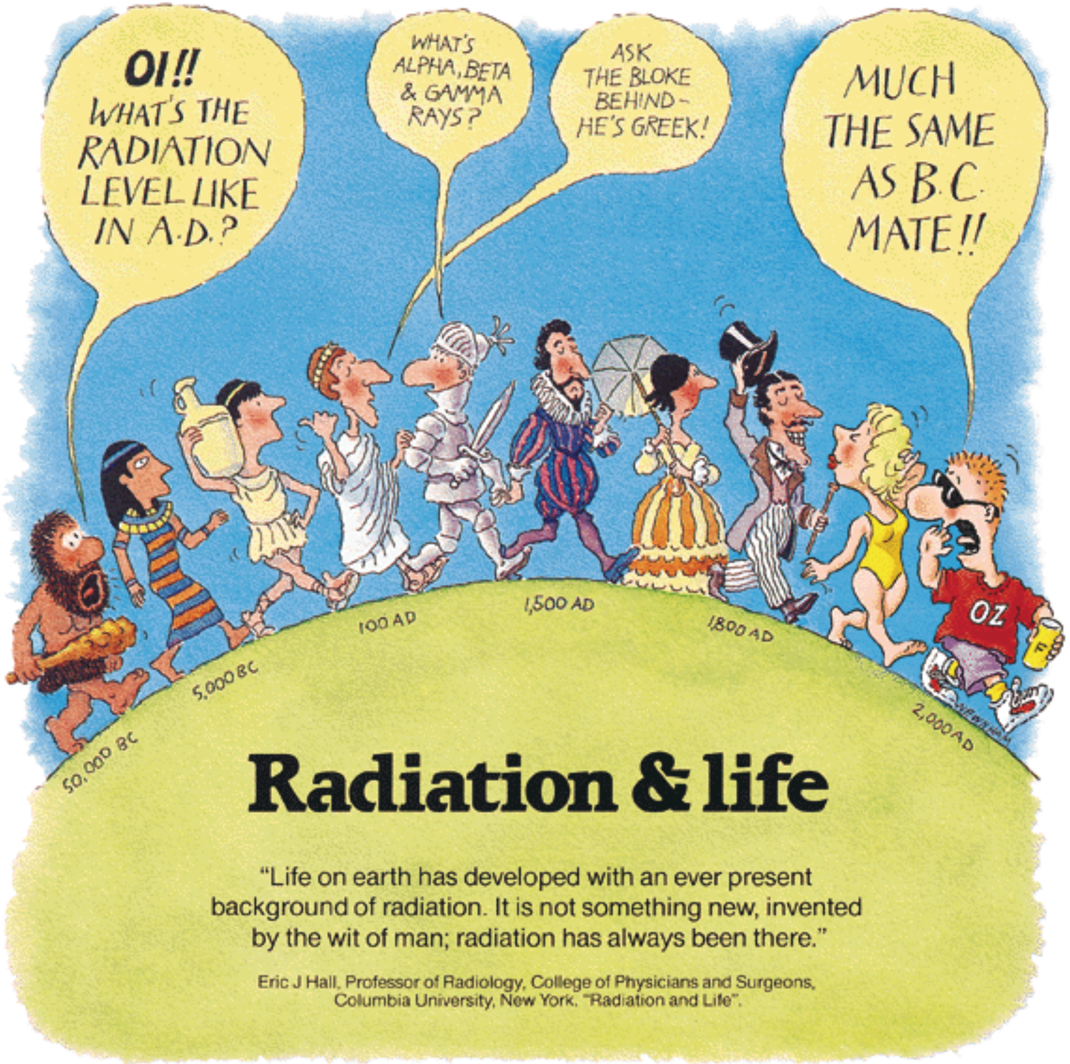
OI!! WHAT'S THE RADIATION LEVEL LIKE IN A.D.?
WHAT'S ALPHA, BETA & GAMMA RAYS?
ASK THE BLOKE BEHIND - HE'S GREEK!
MUCH THE SAME AS B.C. MATE!!
50,000 BC
5,000 BC
100 AD
1,500 AD
1800 AD
2,000 AD
OZ
Radiation & life
"Life on earth has developed with an ever present background of radiation. It is not something new, invented by the wit of man; radiation has always been there."
Eric J Hall, Professor of Radiology, College of Physicians and Surgeons, Columbia University, New York. "Radiation and Life".

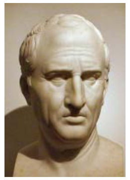

Memoria est thesaurus omnium rerum et custos

Marcus Tullius Cicero, De oratore (1, 5, 18)

The Big…Family

Wilhelm Konrad Röntgen
X Rays (Nobel Prize in Physics 1901)

Antoine Henri Becquerel – Pierre Curie – Marie Skłodowska Curie
Radioactivity (Nobel Prize in Physics 1903)

Joseph John Thomson
Electron (Nobel Prize in Physics 1906)

Ernst Rutherford
α and β Particles (Nobel Prize in Chemistry 1908)

Frederick Soddy
Isotopes (Nobel Prize in Chemistry 1921)

Albert Einstein
Theory of Relativity

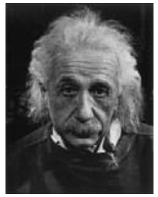

Niels Bohr
Structure of atoms (Nobel Prize in Physics 1922)

Werner Heisenberg
Quantum Mechanics (Nobel Prize in Physics 1932)

Erwin Rudolf Josef Alexander Schrödinger
Quantum Mechanics (Nobel Prize in Physics 1933)

Max Born
Quantum Mechanics (Nobel Prize in Physics 1954)

James Cadwick
Neutron (Nobel Prize in Physics 1935)

Enrico Fermi
Neutron irradiation and nuclear reactions (Nobel Prize in Physics 1938)

Ernest Orlando Lawrence
Cyclotron (Nobel Prize in Physics 1939)

John Douglas Cockcroft - Ernest Thomas Sinton Walton
Transmutation of atomic nuclei (Nobel Prize in Physics 1951)

Hans Albrecht Bethe
Theory of nuclear reactions (Nobel Prize in Physics 1967)

...to be continued

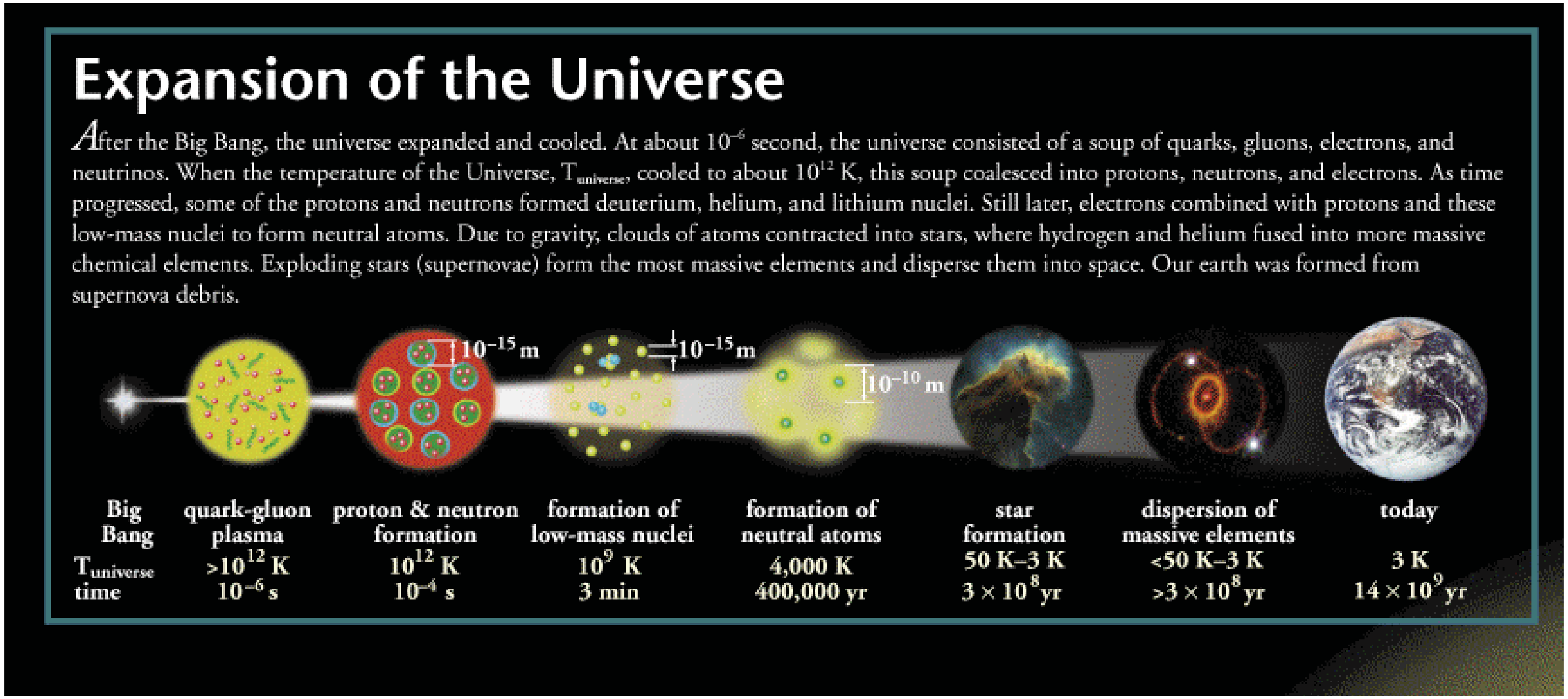
Expansion of the Universe
After the Big Bang, the universe expanded and cooled. At about 10^{-6} second, the universe consisted of a soup of quarks, gluons, electrons, and neutrinos. When the temperature of the Universe, $T_{universe}$, cooled to about 10^{12} K, this soup coalesced into protons, neutrons, and electrons. As time progressed, some of the protons and neutrons formed deuterium, helium, and lithium nuclei. Still later, electrons combined with protons and these low-mass nuclei to form neutral atoms. Due to gravity, clouds of atoms contracted into stars, where hydrogen and helium fused into more massive chemical elements. Exploding stars (supernovae) form the most massive elements and disperse them into space. Our earth was formed from supernova debris.
10^{-15} m
10^{-15} m
10^{-10} m
Big Bang
$T_{universe}$
time
quark-gluon plasma
$>10^{12}$ K
10^{-6} s
proton & neutron formation
10^{12} K
10^{-4} s
formation of low-mass nuclei
10^{9} K
3 min
formation of neutral atoms
4,000 K
400,000 yr
star formation
50 K–3 K
3×10^{8} yr
dispersion of massive elements
<50 K–3 K
$>3 \times 10^{8}$ yr
today
3 K
14×10^{9} yr

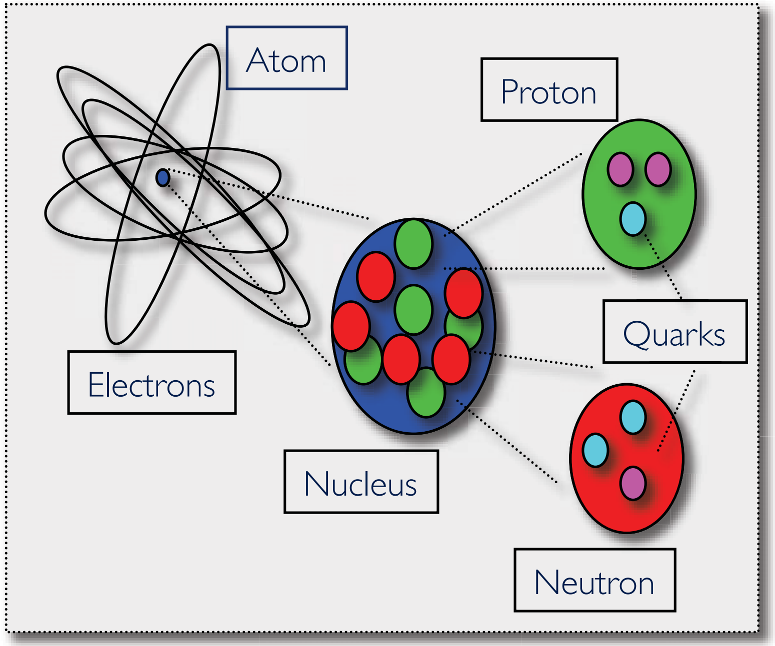
Atom
Proton
Quarks
Electrons
Nucleus
Neutron

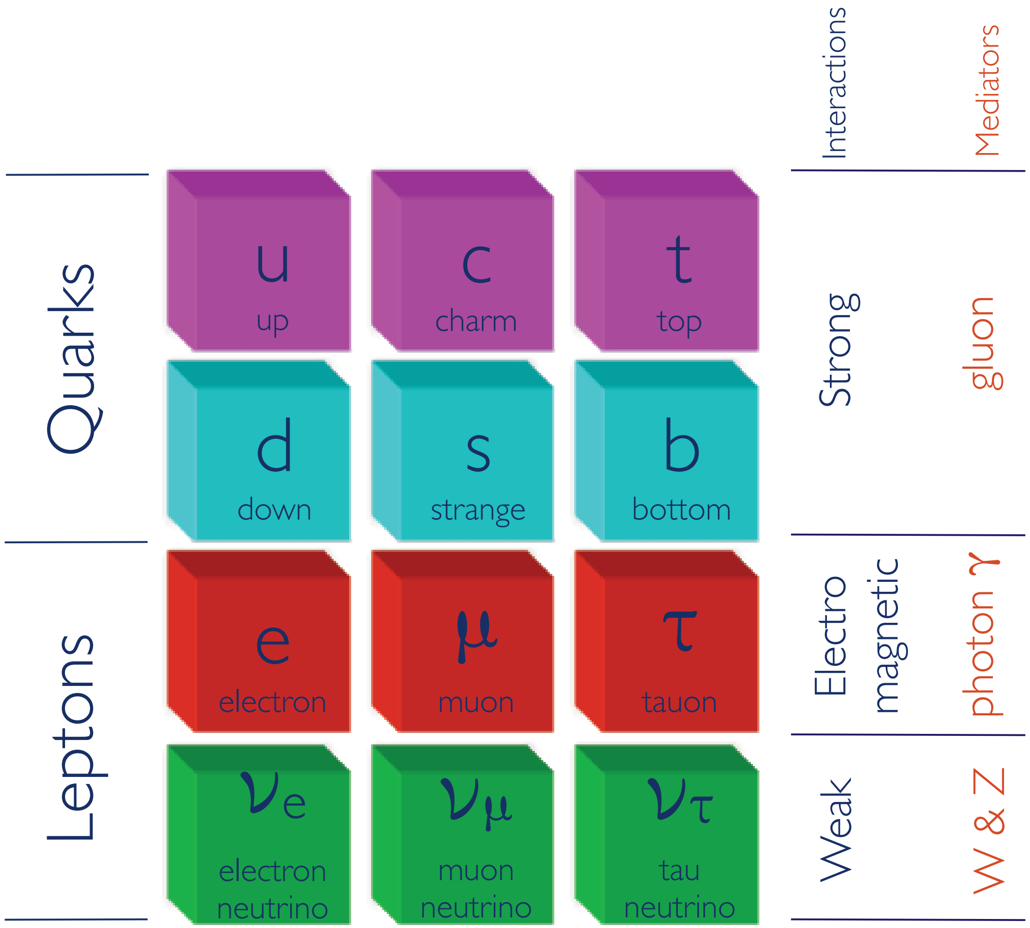
Interactions
Mediators
Quarks
u
up
c
charm
t
top
Strong
gluon
d
down
s
strange
b
bottom
Leptons
e
electron
μ
muon
τ
tauon
Electro
magnetic
photon γ
νe
electron
neutrino
νμ
muon
neutrino
ντ
tau
neutrino
Weak
W & Z

$$^{A}_{Z}X$$

A = number of protons + number of neutrons

Z = number of protons

A – Z = number of neutrons

Number of neutrons = Mass Number – Atomic Number

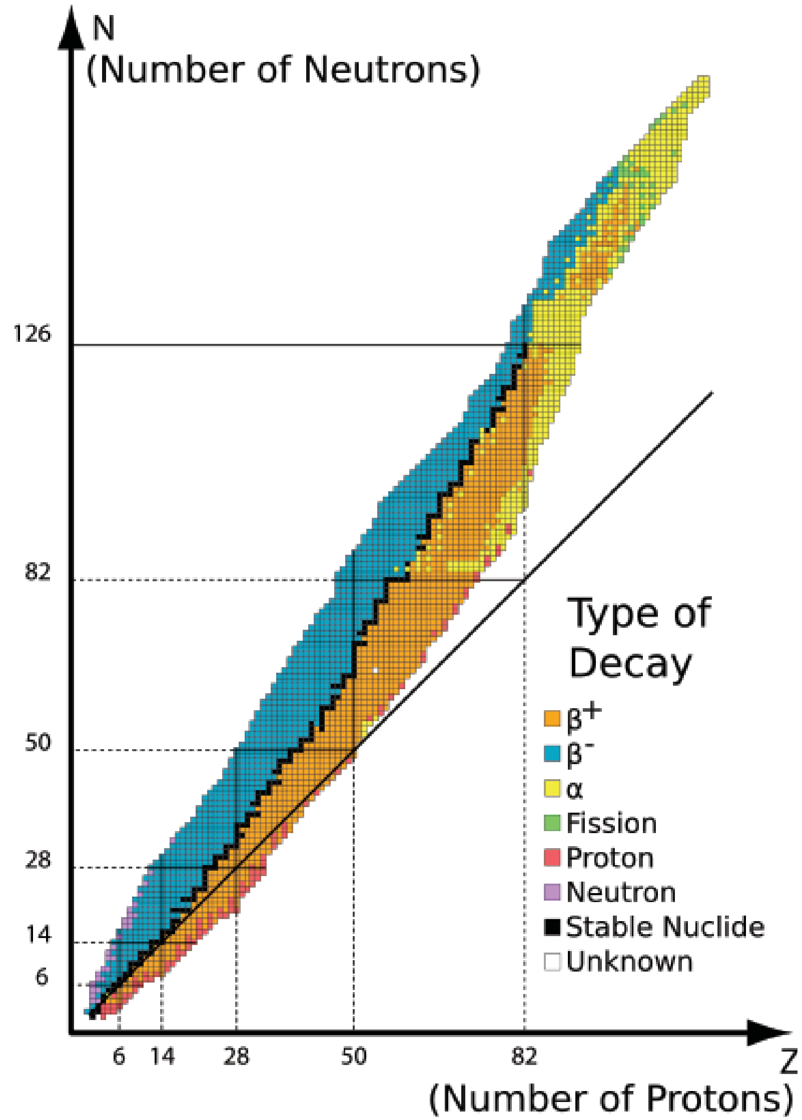

Alpha Decay

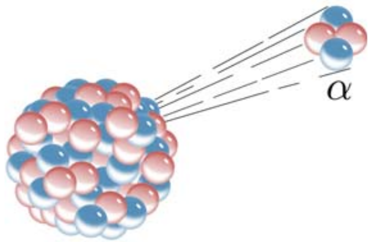

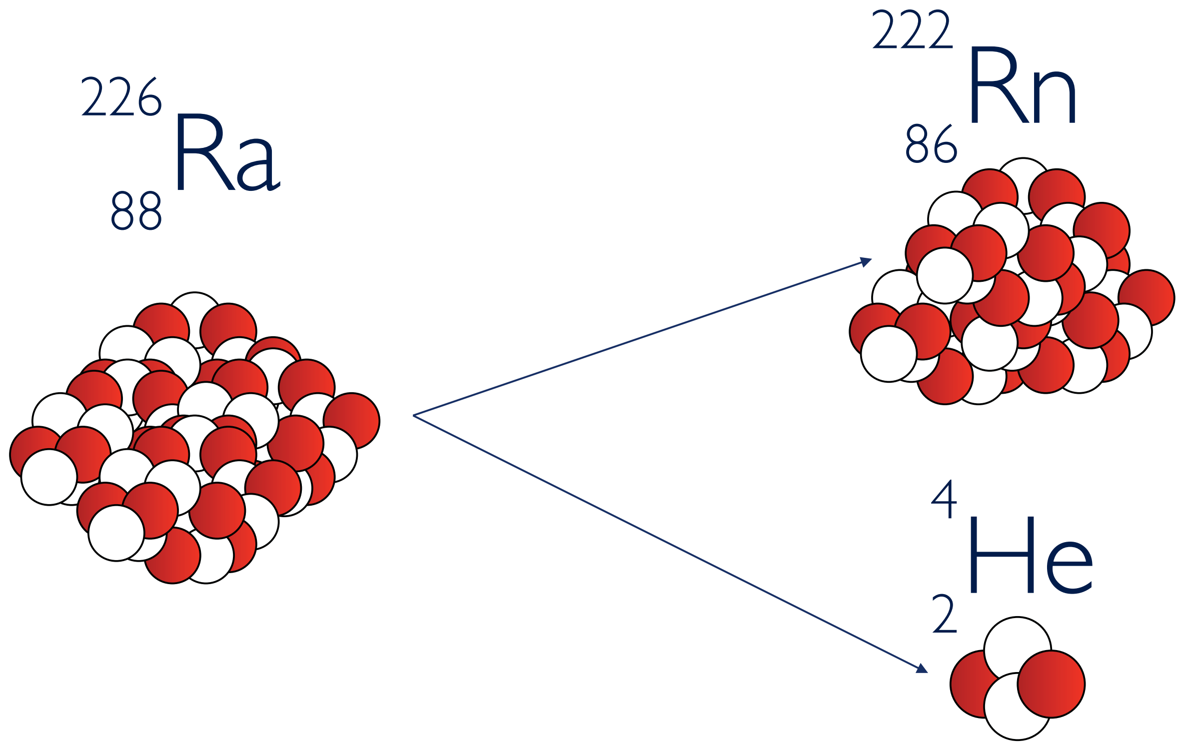

$$^{A}_{Z}X \longrightarrow \, ^{A-4}_{Z-2}Y + \, ^{4}_{2}He$$

Beta Decay (-)

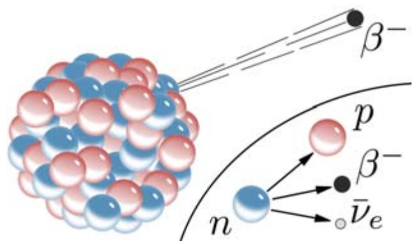

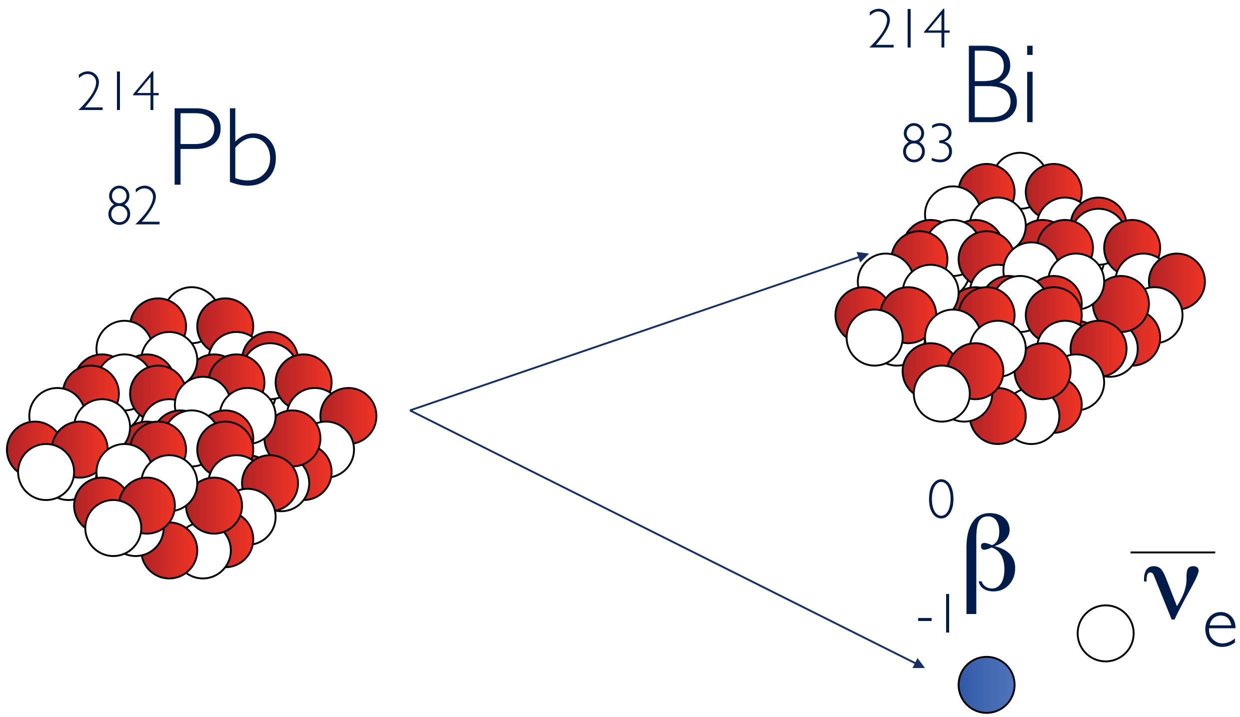

$$^{A}_{Z}X \longrightarrow \, ^{A}_{Z+1}Y + \, ^{0}_{-1}\beta + \bar{\nu}_e$$

Beta Decay (+)

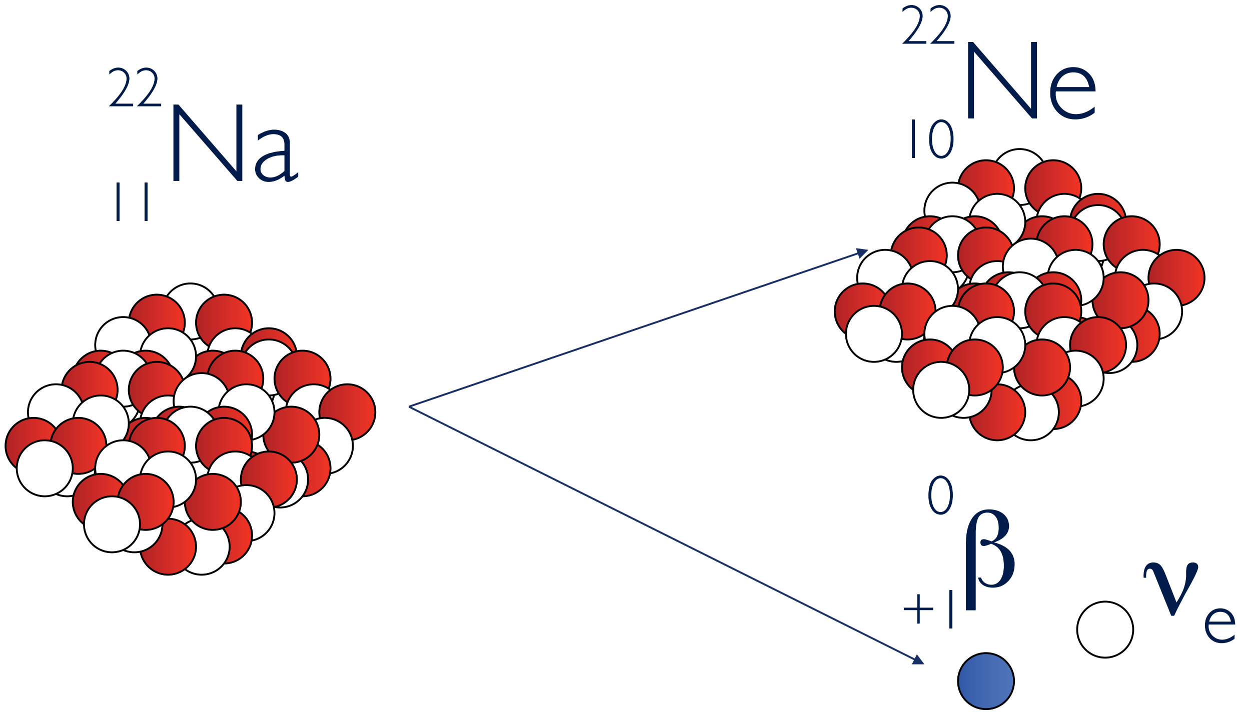

$$^{A}_{Z}X \longrightarrow {}^{A}_{Z-1}Y + {}^{0}_{+1}\beta + \nu_e$$

Gamma Decay

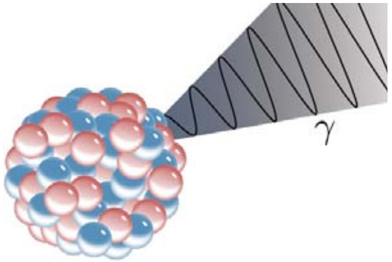

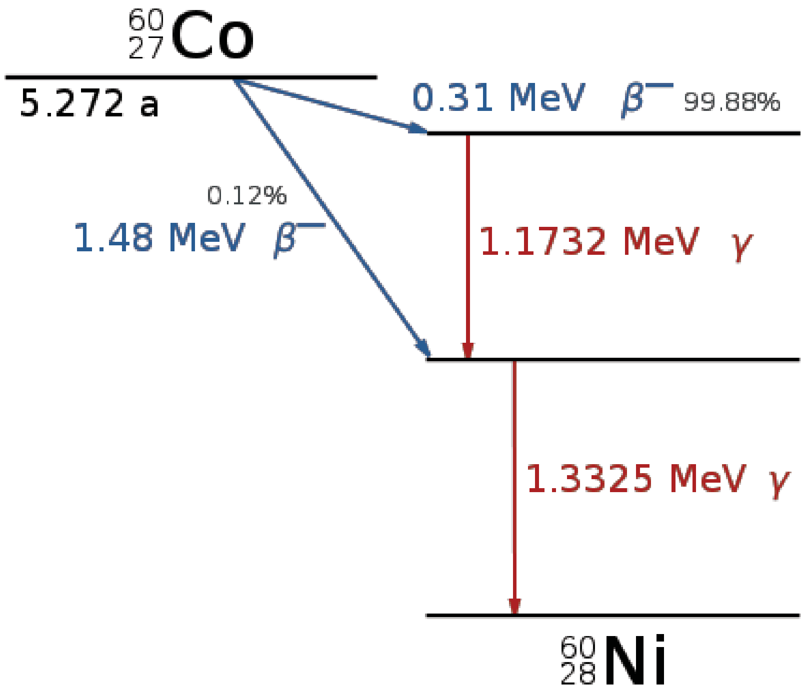

...to be continued

$$N(t) = N_0\, e^{-t/\tau}$$

$$T_{1/2} = \tau \ln 2$$

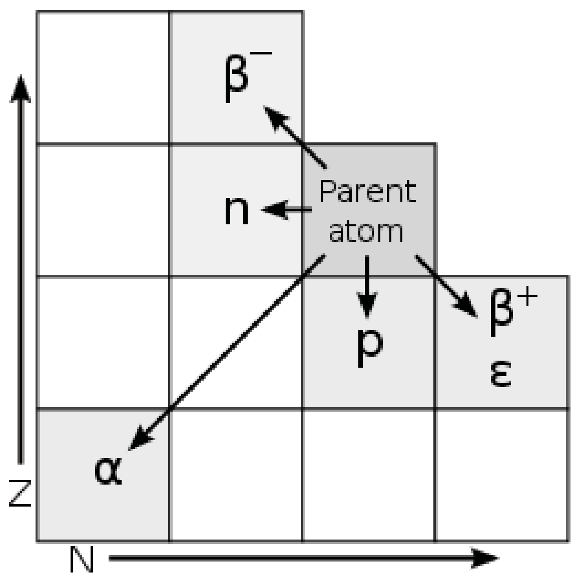

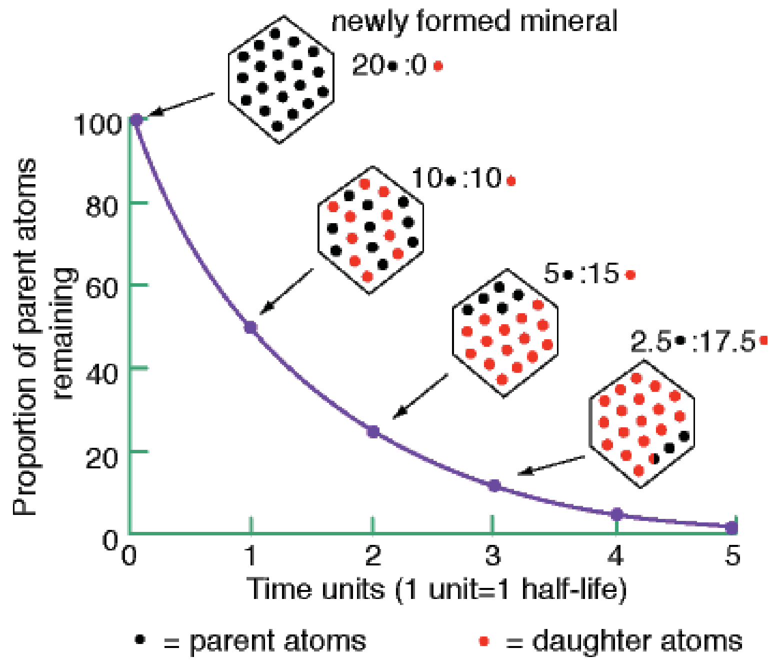

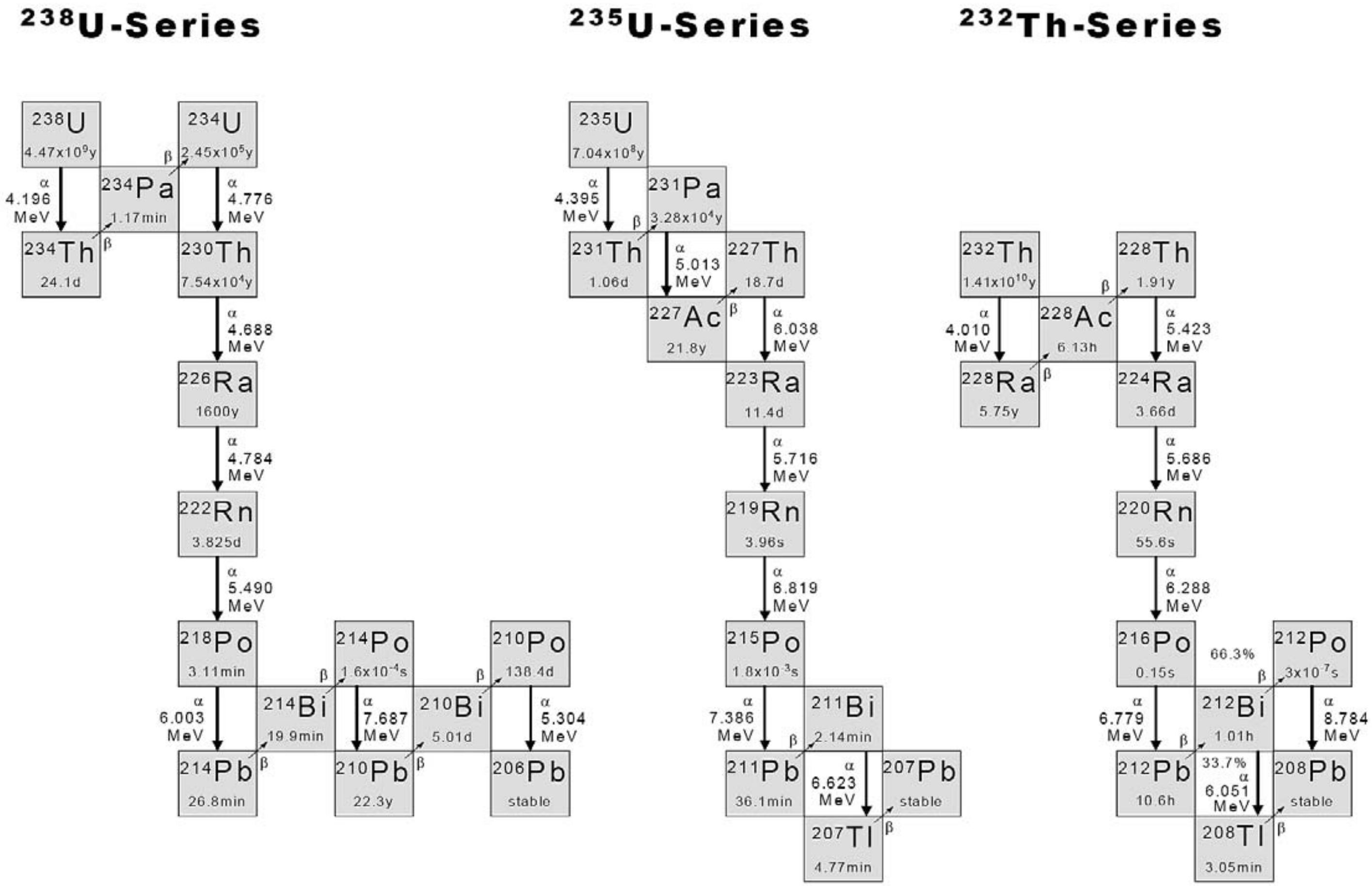

© J. Eikenberg, Paul Scherrer Institute

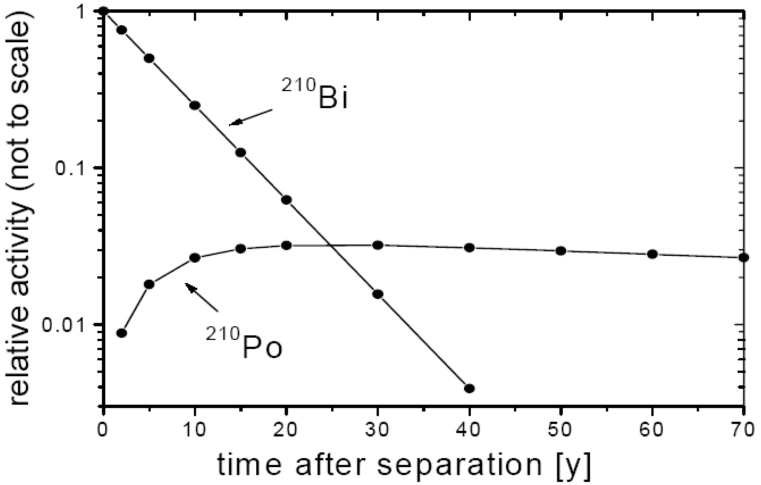
relative activity (not to scale)
time after separation [y]
210Bi
210Po
1
0.1
0.01
0
10
20
30
40
50
60
70

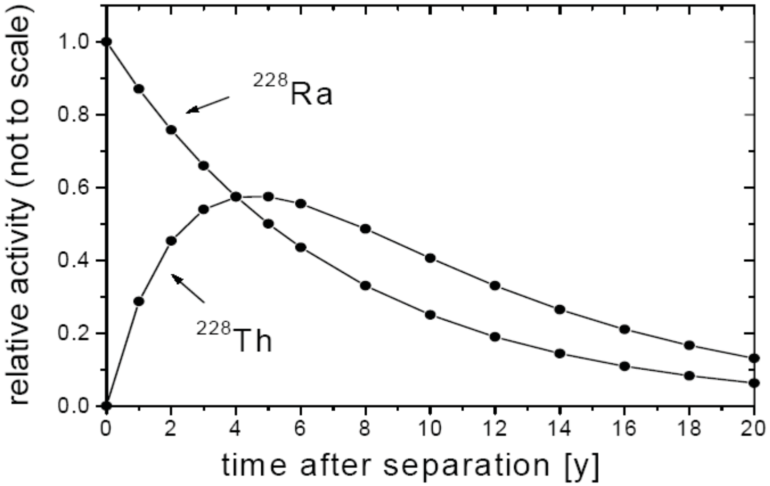
relative activity (not to scale)
time after separation [y]
228Ra
228Th
1.0
0.8
0.6
0.4
0.2
0.0
0
2
4
6
8
10
12
14
16
18
20

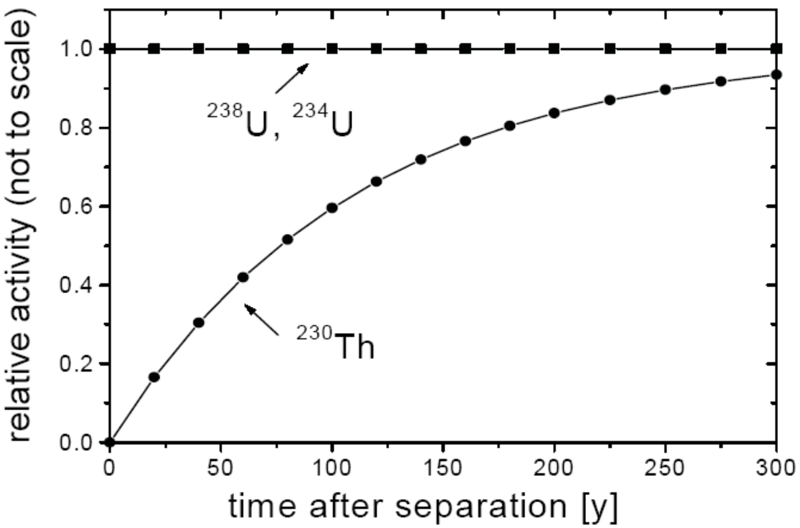
relative activity (not to scale)
time after separation [y]
238U, 234U
230Th
1.0
0.8
0.6
0.4
0.2
0.0
0
50
100
150
200
250
300

type of sample		^{238}U		^{232}Th		^{226}Ra (1)	
		[ppm]	[mBq/g]	[ppm]	[mBq/g]	[ppt]	[mBq/g]
igneous	granite	2 - 10	25 - 120	5 - 30	20 - 120	0.5 - 4	25 - 120
	Gabbro	0.5 - 2	5 - 25	2 - 6	5 - 25	0.1 - 0.5	5 - 25
	Basalt	0.1 - 1	1 - 10	0.3 - 4	1 - 15	0.02 - 0.2	1 - 10
	Ultramafics	< 0.02	< 0.2	< 0.05	< 0.2	< 0.01	< 0.2
sedimentary	Shales	2 - 4	25 - 50	5 - 15	20 - 120	0.5 - 1	25 - 50
	Limestone	1 - 3	10 - 40	0 - 3	0 - 10	0.2 - 1	10 - 40
	Speleothem	1 - 3	10 - 40	0 - 3	0 - 10	0.2 - 1	10 - 40
	Coral	2 - 4	25 - 50	< 0.01	<0.04	0.5 - 1	25 - 50
	Clay	1 - 4	10 - 50	1 - 15	5 - 60	0.2 - 1	10 - 50
water (2)	sea water (3)	3 - 4	40 - 50	< 0.01	< 0.05	0.01 - 0.1	0.5 – 5
	river water (4)	0.1 - 1	1 - 10	< 0.01	< 0.05	0.01 - 0.1	0.5 – 5

Detector type	Principle of detection	Type of radiation	Sample source	Geometry, maximum detector efficiency	MDA [Bq/l]
α-spectrometer	semiconductive material (Si)	α, (β)	planar disc	2π, 40%(α)	$4 \cdot 10^{-4}$ (a)
γ-spectrometer	semiconductive material (Ge)	γ, X-ray	direct sample measurement	2π, 10% (1)	$5 \cdot 10^{-2}$ (b)
NaI-Detektor	solid scintillator (NaI crystal)	γ, X-ray	direct sample measurement	2π, 30% (2)	$5 \cdot 10^{-2}$ (b)
α/β proportional counter	counting gas ionization	α, β	planar disc	2π, 45(β), 30(α)	$1 \cdot 10^{-3}$ (a)
grid ionization chamber	counting gas ionization	α, (β)	planar disc	2π, 30%(α)	$4 \cdot 10^{-3}$ (c)
α/β liquid scint. spectrometer	liquid scintillator	α, β	scintillation cocktail	2π, 100%(α+β)	$1 \cdot 10^{-2}$ (d)

(1) valid for a 30% efficiency intrinsic Ge detector (relative to 3x3' NaI) using a 3 cm planar source measured on the detector surface and for a photon energy of 200 keV

(2) valid for a 3x3' ∅ NaI-Detector using a 3 cm planar source measured on the detector surface and for a photon energy of 200 keV

(a) radiochemical separation (sorption onto MnO_2-coated discs) from a 1 liter sample

(b) measurement of the ^{222}Rn progenies ^{214}Pb, ^{214}Bi in gas tight containers (6 liter simultaneously)

(c) evaporation of 100 ml water in a large surface (20 cm ∅) sample holder

(d) extraction of ^{222}Rn from a 100 ml water sample into an organic cocktail using a separation funnel

isotope	origin	mode of decay	mode of detection	detection limit [Bq/g]	detection limit [g/g]
^{238}U	^{238}U-series	α, (γ)	α-spectrometry	$5 \cdot 10^{-5}$	$4 \cdot 10^{-9}$
^{235}U	^{235}U-series	α, γ	α-spectrometry	$5 \cdot 10^{-5}$	$6 \cdot 10^{-10}$
^{234}U	^{238}U-series	α, (γ)	α-spectrometry	$5 \cdot 10^{-5}$	$2 \cdot 10^{-13}$
^{236}U	*spike isotope*	α, (γ)	α-spectrometry	$5 \cdot 10^{-5}$	$8 \cdot 10^{-11}$
^{233}U	*spike isotope*	α, (γ)	α-spectrometry	$5 \cdot 10^{-5}$	$1 \cdot 10^{-13}$
^{232}U	*spike isotope*	α, (γ)	α-spectrometry	$5 \cdot 10^{-5}$	$6 \cdot 10^{-17}$
^{231}Pa	^{235}U-series	α, (γ)	α-spectrometry	$5 \cdot 10^{-5}$	$3 \cdot 10^{-14}$
^{233}Pa	*spike isotope*	β, γ	γ-spectrometry	$1 \cdot 10^{-1}$	$1 \cdot 10^{-16}$
^{232}Th	^{232}Th-series	α, (γ)	α-spectrometry	$5 \cdot 10^{-5}$	$1 \cdot 10^{-8}$
^{230}Th	^{238}U-series	α, (γ)	α-spectrometry	$5 \cdot 10^{-5}$	$7 \cdot 10^{-14}$
^{228}Th	^{232}Th-series	α, (γ)	α-spectrometry	$5 \cdot 10^{-5}$	$2 \cdot 10^{-18}$
^{229}Th	*spike isotope*	α, (γ)	α-spectrometry	$5 \cdot 10^{-5}$	$5 \cdot 10^{-14}$
^{228}Ra	^{232}Th-series	β	proportional counting	$1 \cdot 10^{-3}$	$1 \cdot 10^{-16}$
^{226}Ra	^{238}U-series	α (γ)	α-spectrometry	$5 \cdot 10^{-5}$	$1 \cdot 10^{-15}$
^{226}Ra	^{238}U-series	α, (γ)	α/β-LSC	$5 \cdot 10^{-4}$	$1 \cdot 10^{-14}$
^{224}Ra	^{232}Th-series	α, (γ)	α-spectrometry	$1 \cdot 10^{-4}$	$2 \cdot 10^{-20}$
^{223}Ra	^{235}U-series	α, (γ)	α-spectrometry	$5 \cdot 10^{-5}$	$3 \cdot 10^{-20}$
^{210}Pb	^{238}U-series	β, (γ)	proportional counting	$1 \cdot 10^{-3}$	$3 \cdot 10^{-16}$
^{210}Pb	^{238}U-series	β, (γ)	α/β-LSC	$5 \cdot 10^{-3}$	$2 \cdot 10^{-15}$
^{210}Po	^{238}U-series	α	α-spectrometry	$5 \cdot 10^{-5}$	$3 \cdot 10^{-19}$
^{209}Po	*spike isotope*	α	α-spectrometry	$5 \cdot 10^{-5}$	$6 \cdot 10^{-17}$
^{208}Po	*spike isotope*	α	α-spectrometry	$5 \cdot 10^{-5}$	$3 \cdot 10^{-18}$

...to be continued

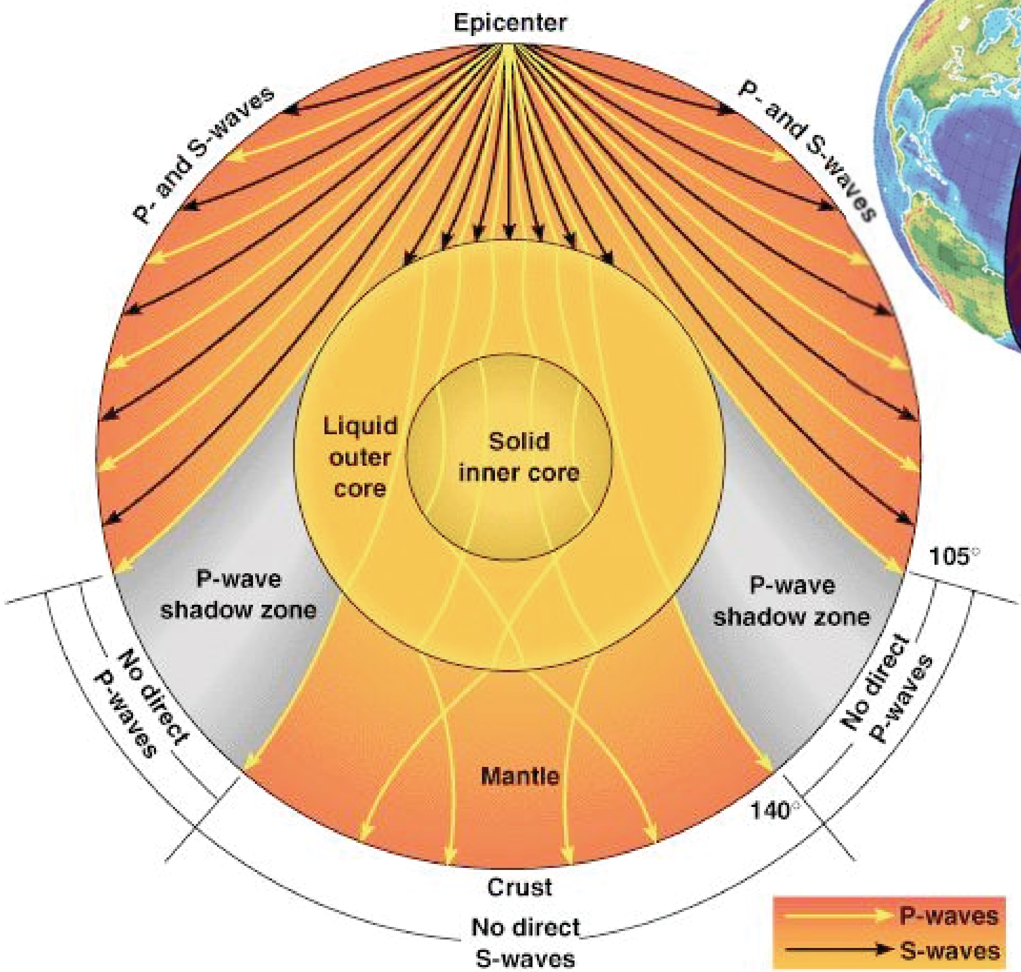
Epicenter
P- and S-waves
P- and S-waves
Liquid
outer
core
Solid
inner core
P-wave
shadow zone
P-wave
shadow zone
105°
No direct
P-waves
No direct
P-waves
Mantle
140°
Crust
No direct
S-waves
P-waves
S-waves

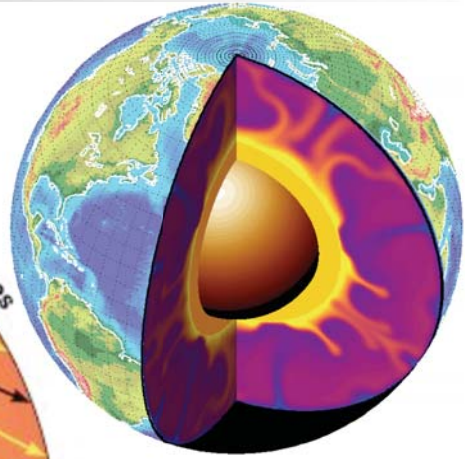


KTB

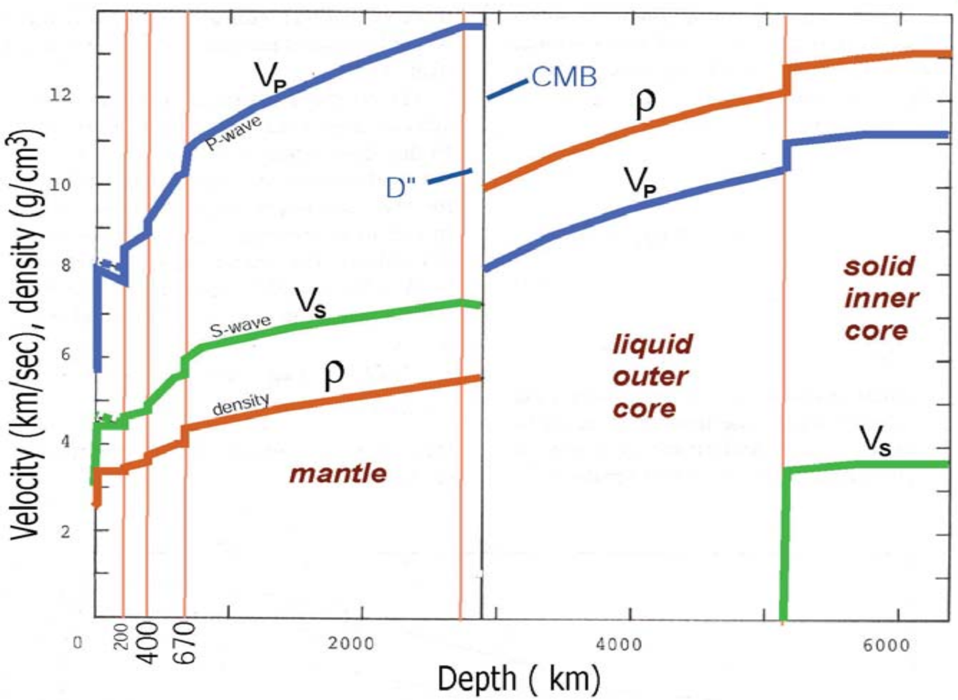
Velocity (km/sec), density (g/cm³)
Depth (km)
0
200
400
670
2000
4000
6000
2
4
6
8
10
12
V_P
P-wave
CMB
D"
ρ
V_P
S-wave
V_S
density
ρ
mantle
liquid
outer
core
solid
inner
core
V_S

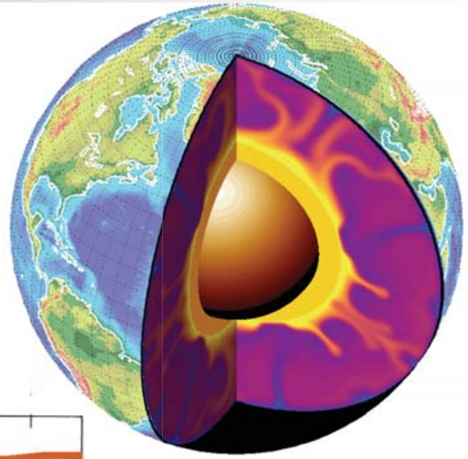

"Energetics of the Earth and the missing heat source mistery" *

- Heat flow from the Earth is the equivalent of some 10000 nuclear power plants

$$H_{Earth} = (30 - 44)\,TW$$

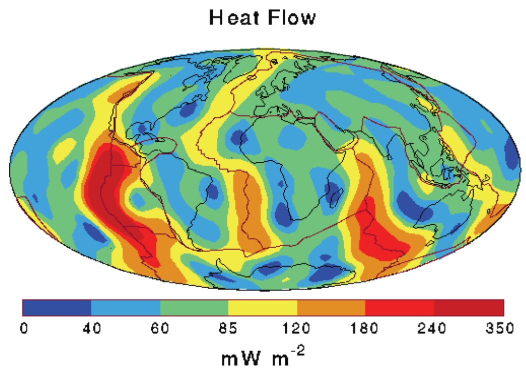

- The BSE canonical model, based on cosmochemical arguments, predicts a radiogenic heat production ~ 19 TW:
  ~ 9 TW estimated from radioactivity in the (continental) crust
  ~ 10 TW supposed from radioactivity in the mantle
  ~ 0 TW assumed from the core

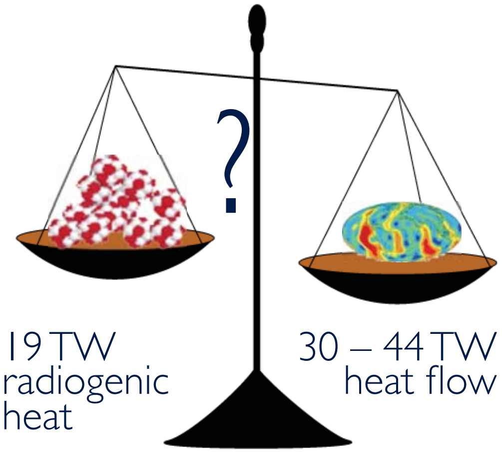

- Unorthodox or even heretical models have been advanced…

* D. L. Anderson (2005), Technical Report, www.MantlePlume.org

"Energetics of the Earth and the missing heat source mistery" *

- Heat flow from the Earth is the equivalent of some 10000 nuclear power plants

$$H_{Earth} = (30 - 44) TW$$

- The BSE canonical model, based on cosmochemical arguments, predicts a radiogenic heat production ~ 19 TW:
~ 9 TW estimated from radioactivity in the (continental) crust
~ 10 TW supposed from radioactivity in the mantle
~ 0 TW assumed from the core

- Unorthodox or even heretical models have been advanced…

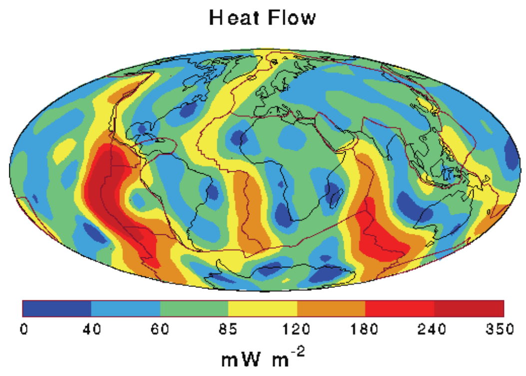

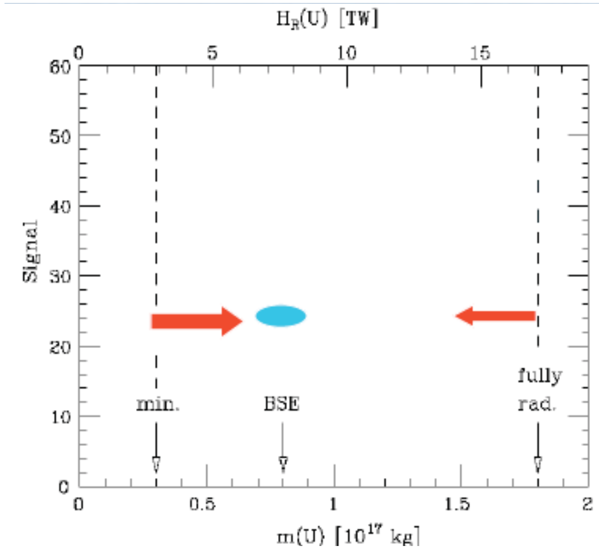

* D. L. Anderson (2005), Technical Report, www.MantlePlume.org

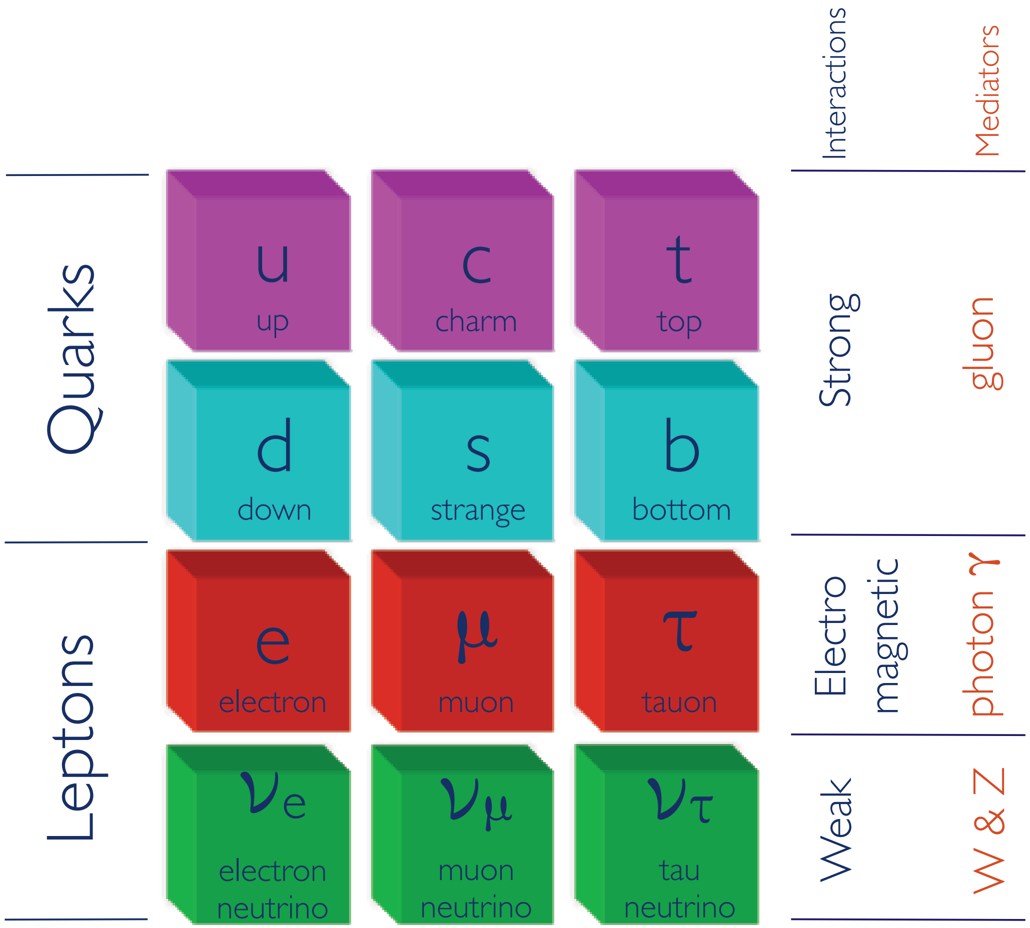
Quarks
Leptons
u
up
c
charm
t
top
d
down
s
strange
b
bottom
e
electron
μ
muon
τ
tauon
νe
electron neutrino
νμ
muon neutrino
ντ
tau neutrino
Interactions
Mediators
Strong
gluon
Electro magnetic
photon γ
Weak
W & Z

Where do Neutrinos come from?

Nuclear Reactors (power stations, ships) and Nuclear Weapons

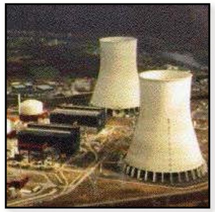

Sun

Particle Accelerator

CERN

Supernovae (star collapse) SN 1987A

Earth's Atmosphere (Cosmic Rays)

Astrophysical Accelerators Soon ?

Earth's Crust (Natural Radioactivity)

Big Bang (here 330 ν/cm^3) Indirect Evidence

Decay	$T_{1/2}$ [10^9 yr]
$^{238}U \rightarrow {}^{206}Pb + 8\,{}^4He + 6e + 6\bar{\nu}$	4.47
$^{232}Th \rightarrow {}^{208}Pb + 6\,{}^4He + 4e + 4\bar{\nu}$	14.0
$^{40}K \rightarrow {}^{40}Ca + e + \bar{\nu}$ (89%)	1.28

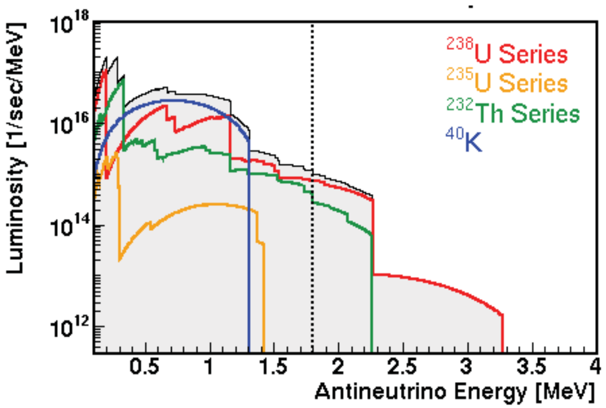

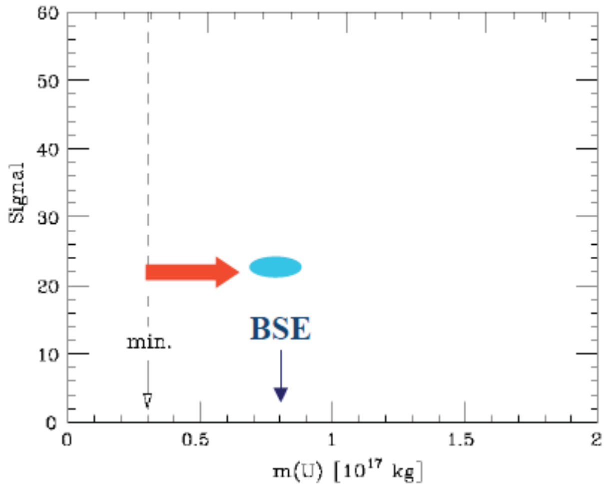

Earth emits (mainly) antineutrinos (10^6 cm^{-2} s^{-1}) whereas Sun shines in neutrinos

A fraction of geo-neutrinos from U and Th (not from ^{40}K) are above threshold for inverse β on protons

© BOREXINO

Geo-neutrino signal and radiogenic heat from the Earth

 region allowed by BSE: signal between 31 and 43 TNU

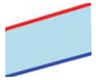 region containing all models consistent with geochemical and geophysical data

U and Th measured in the crust implies a signal at least of 24 TNU

Earth energetics implies the signal does not exceed 62 TNU

Fiorentini et al. (2005)

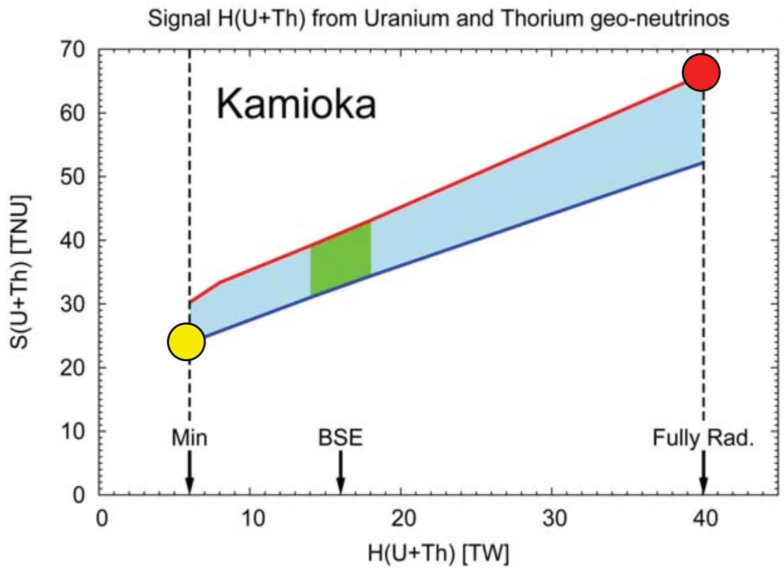

The graph is site dependent:

- ✓ the "slope" is universal
- ✓ the intercept depends on the site (crust effect)
- ✓ the width depends on the site (crust effect)

1 TNU = one event per 10^{32} free protons per year

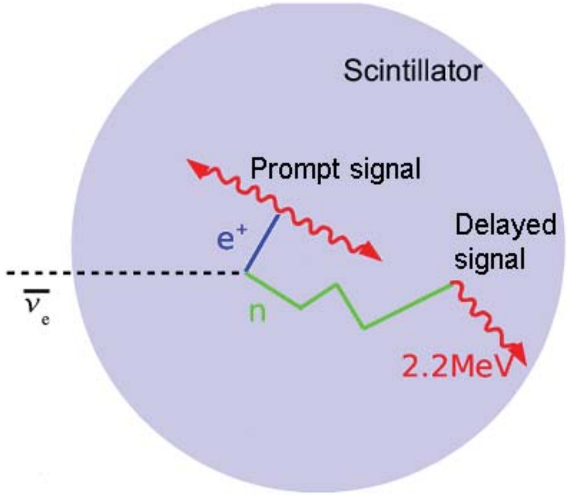

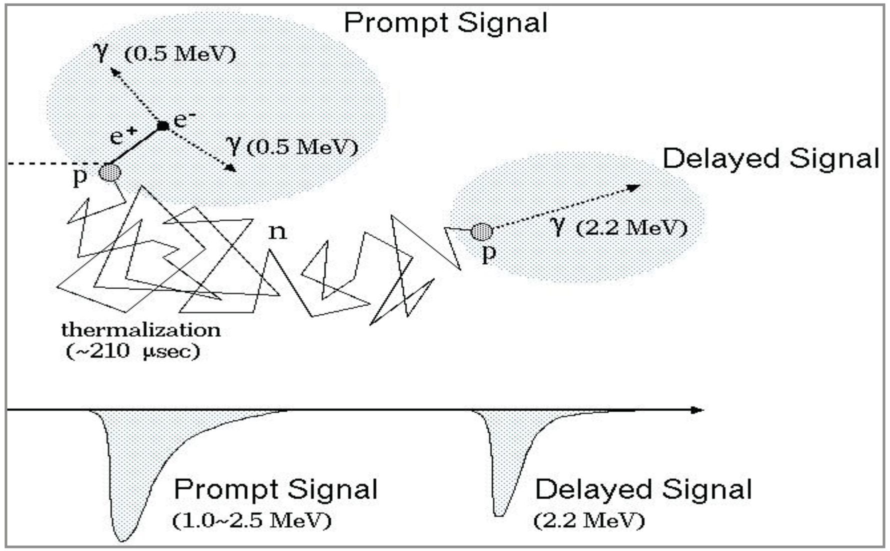

...to be continued

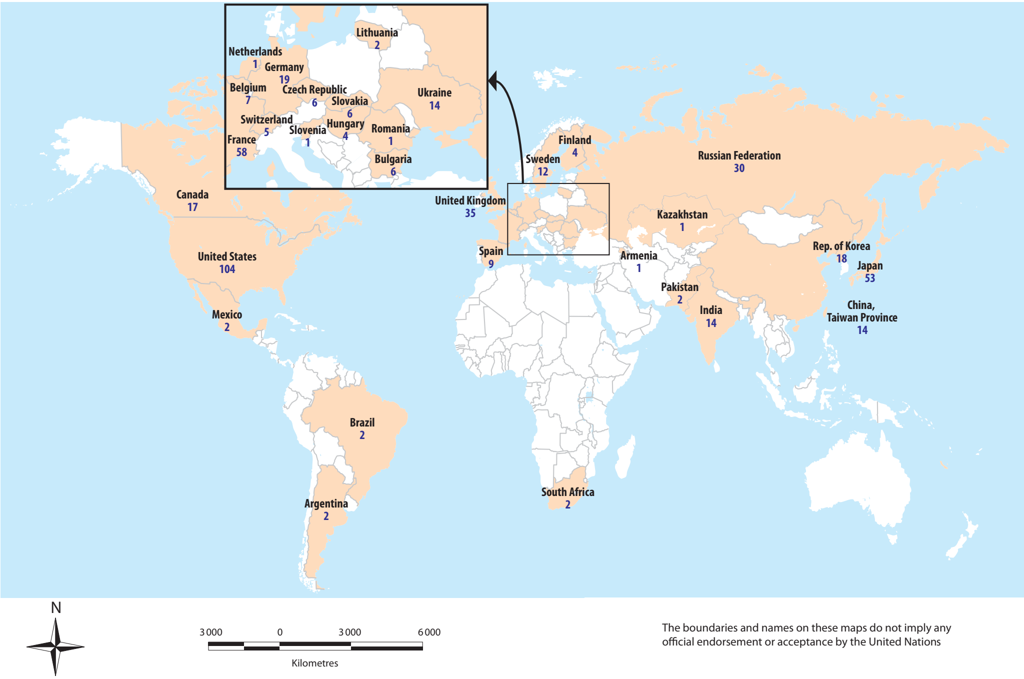
Lithuania 2
Netherlands 1
Germany 19
Belgium 7
Czech Republic 6
Slovakia 6
Ukraine 14
Switzerland 5
Slovenia 1
Hungary 4
Romania 1
France 58
Bulgaria 6
Finland 4
Sweden 12
Russian Federation 30
Canada 17
United Kingdom 35
Kazakhstan 1
United States 104
Spain 9
Armenia 1
Rep. of Korea 18
Japan 53
Pakistan 2
Mexico 2
India 14
China, Taiwan Province 14
Brazil 2
South Africa 2
Argentina 2
N
3 000 0 3 000 6 000
Kilometres
The boundaries and names on these maps do not imply any official endorsement or acceptance by the United Nations

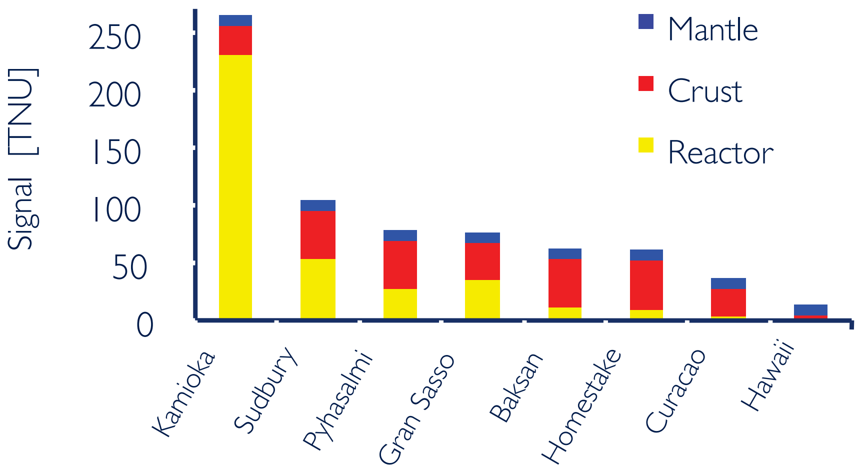
Signal [TNU]
0
50
100
150
200
250
Kamioka
Sudbury
Pyhasalmi
Gran Sasso
Baksan
Homestake
Curacao
Hawaii
Mantle
Crust
Reactor

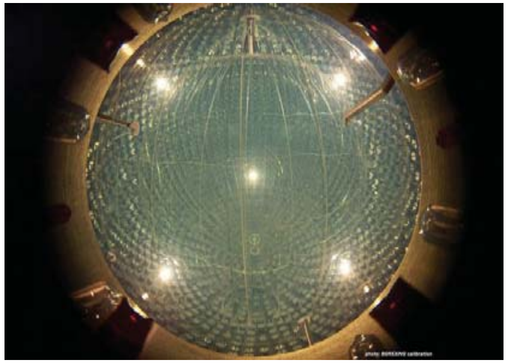

Borexino at Gran Sasso

- A 300-ton liquid scintillator underground detector, running since may 2007.

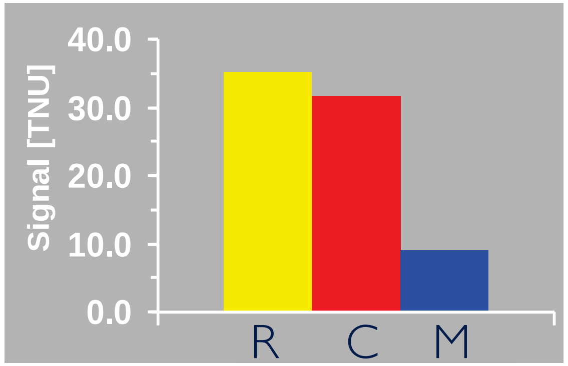

- Signal, mainly generated from the crust, is comparable to reactor background.

- From BSE expect 5 – 7 events/year*

- In about two years should get 3σ evidence of geo-neutrinos.

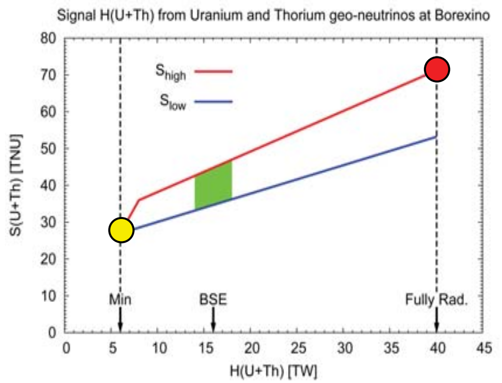

* For 80% eff. and 300 tons C_9H_{12} fiducial mass

Borexino collaboration - European Physical Journal C 47 21 (2006) - arXiv:hep-ex/0602027

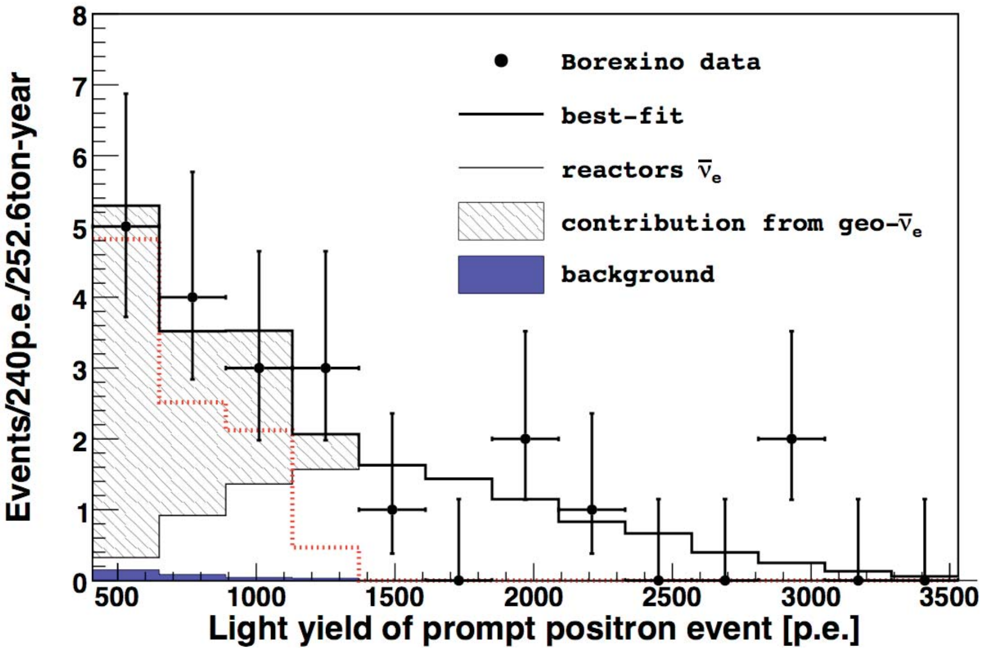
Borexino data
best-fit
reactors $\bar{\nu}_e$
contribution from geo-$\bar{\nu}_e$
background
Events/240p.e./252.6ton-year
Light yield of prompt positron event [p.e.]

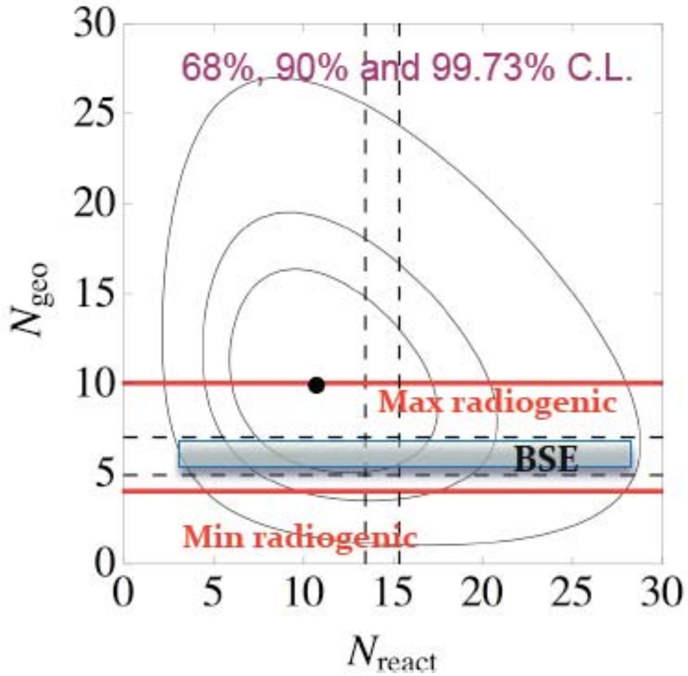
68%, 90% and 99.73% C.L.
Max radiogenic
BSE
Min radiogenic
N_{geo}
N_{react}

SNO+ at Sudbury

- A 1000-ton liquid scintillator underground detector, obtained by replacing D_2O in SNO.
- The SNO collaboration has planned to fill the detector with LS in 2009

- 80% of the signal comes from the continental crust.
- From BSE expect 28 – 38 events/year*
- It should be capable of measuring U+Th content of the crust.

* assuming 80% eff. and 1 kTon CH_2 fiducial mass

Chen, M. C., 2006, Earth Moon Planets 99, 221.

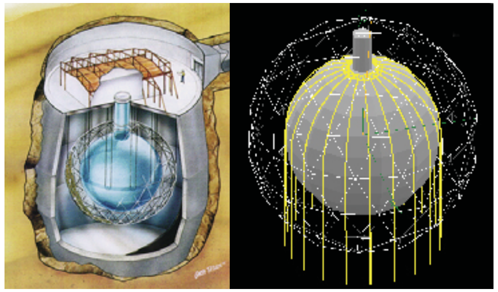

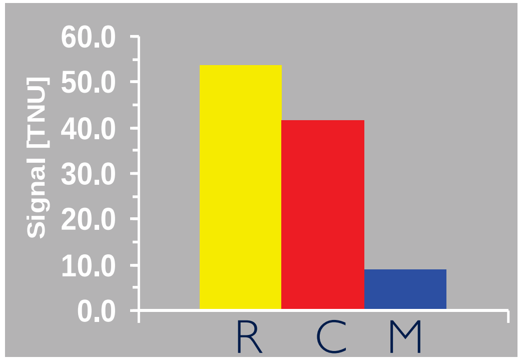

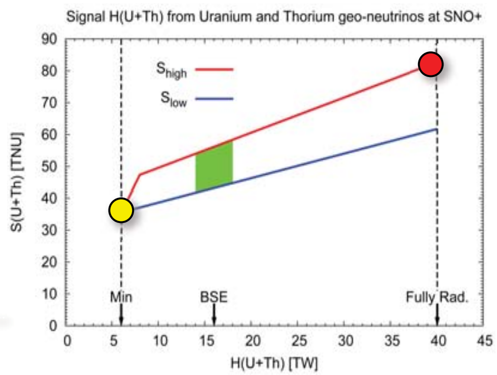

Hanohano at Hawaii

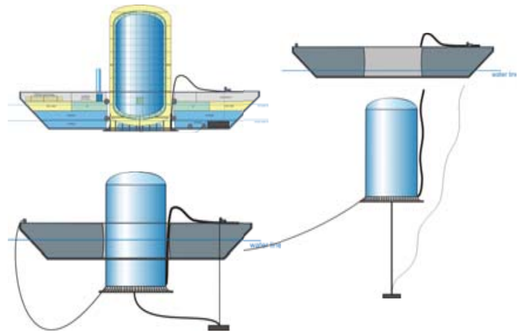

- Project of a 10 kiloton movable deep-ocean LS detector
- ~ 70% of the signal comes from the mantle
- From BSE expect 60 – 100 events/year*
- It should be capable of measuring U+Th content of the mantle

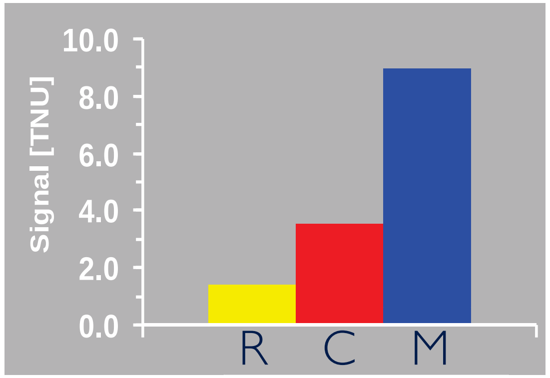

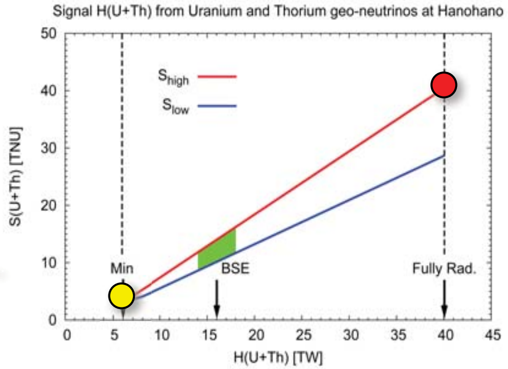

* assuming 80% eff. and 10 kTon CH_2 fiducial mass

J. G. Learned et al. – ``XII-th International Workshop on Neutrino Telescope'', Venice, 2007

LENA at Pyhasalmi

- Project of a 50 kiloton underground liquid scintillator detector in Finland
- 80% of the signal comes from the crust
- From BSE expect 800 – 1200 events/year*
- LS is loaded with 0.1% Gd which provides:
  - better neutron identification
  - moderate directional information

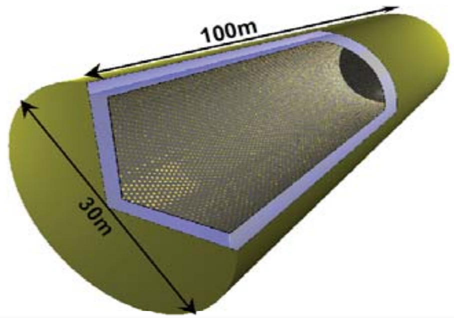

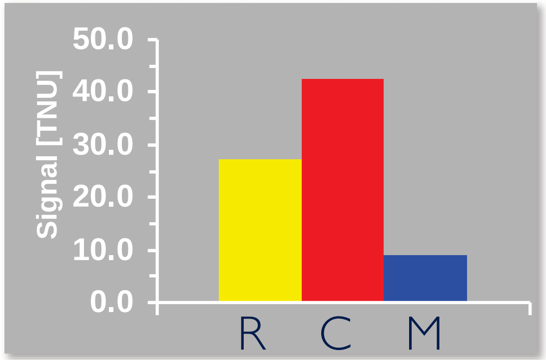

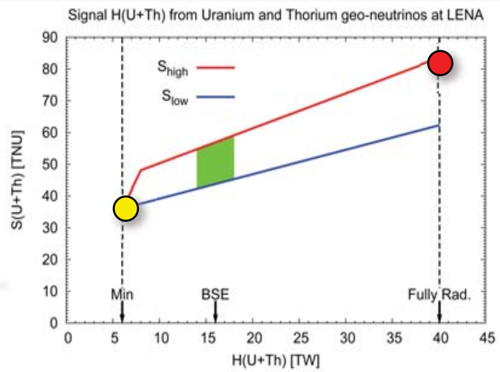

* For 2.5 10^{33} free protons and assuming 80% eff.

K. A. Hochmuth et al. - Astropart.Phys. 27 (2007) - arXiv:hep-ph/0509136 ; Teresa Marrodan @Taup 2007

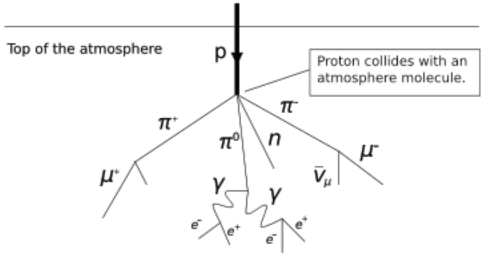
Top of the atmosphere
p
Proton collides with an atmosphere molecule.
π^+
π^-
π^0
n
μ^+
μ^-
$\bar{\nu}_\mu$
γ
γ
e^-
e^+
e^-
e^+

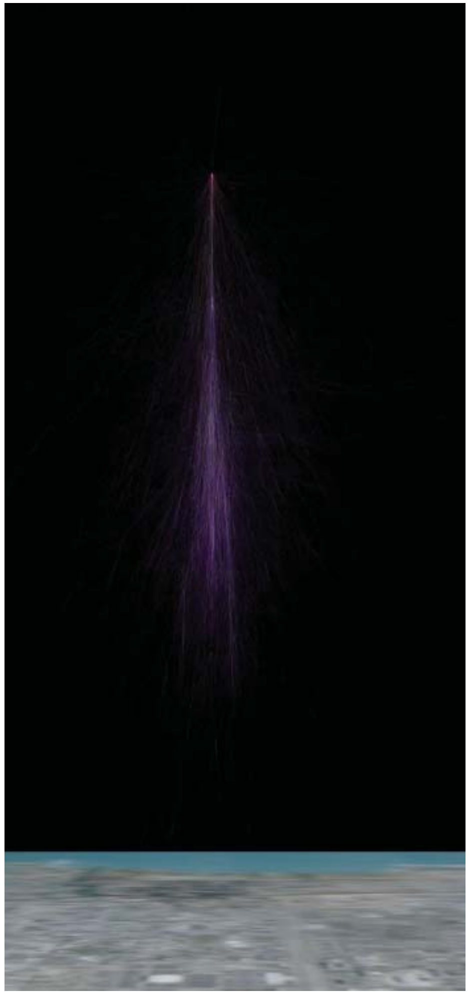

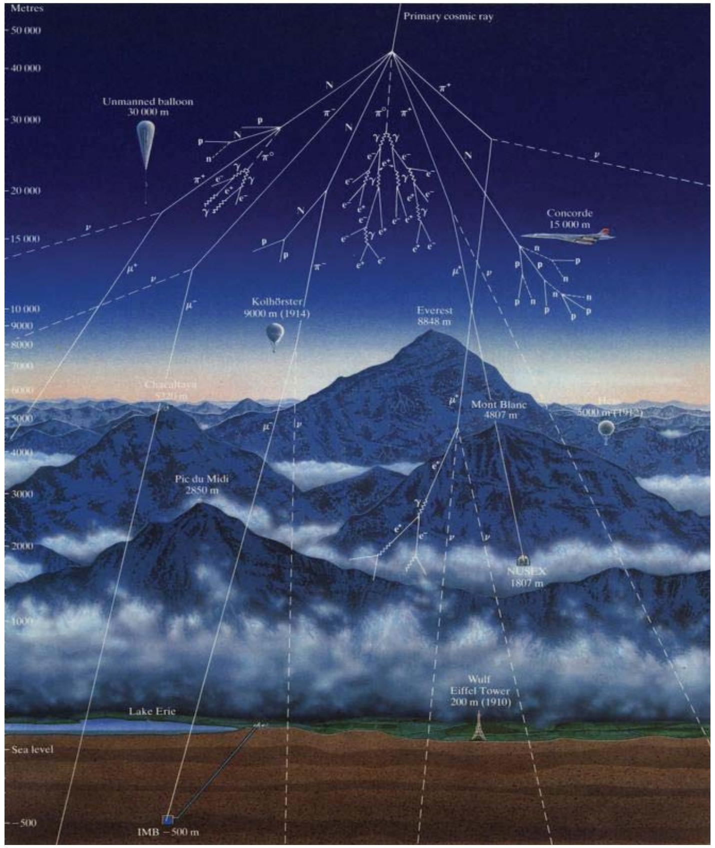
Metres
Primary cosmic ray
Unmanned balloon
30 000 m
Concorde
15 000 m
Kolhörster
9000 m (1914)
Everest
8848 m
Mont Blanc
4807 m
Pic du Midi
2850 m
NUSEX
1807 m
Wulf
Eiffel Tower
200 m (1910)
Lake Erie
Sea level
IMB – 500 m

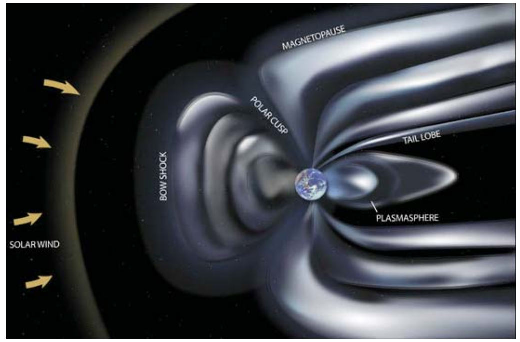
MAGNETOPAUSE
POLAR CUSP
TAIL LOBE
BOW SHOCK
PLASMASPHERE
SOLAR WIND

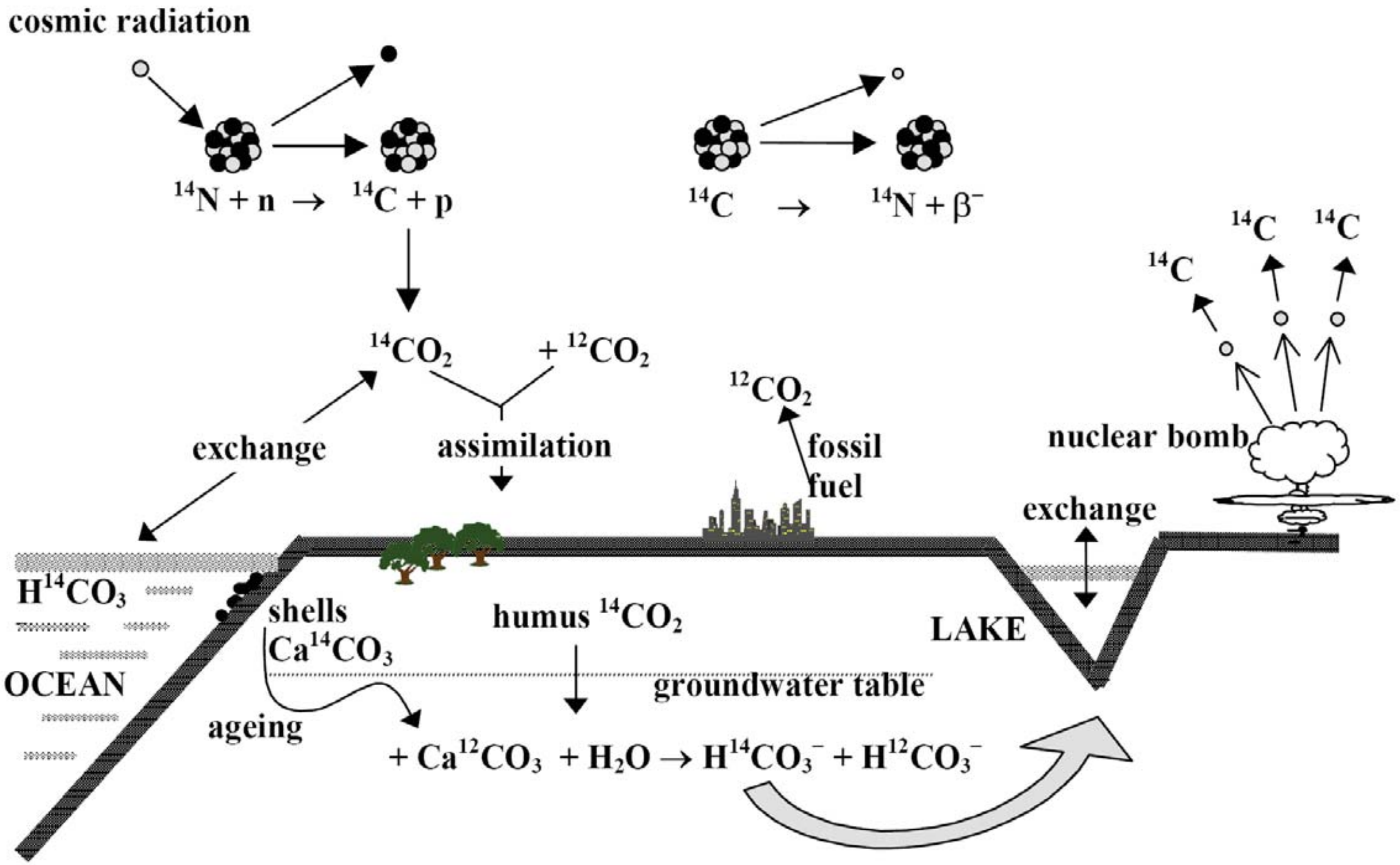
cosmic radiation
$^{14}N + n \rightarrow {}^{14}C + p$
$^{14}C \rightarrow {}^{14}N + \beta^-$
^{14}C
^{14}C
^{14}C
$^{14}CO_2$
$+ {}^{12}CO_2$
$^{12}CO_2$
exchange
assimilation
fossil
fuel
nuclear bomb
exchange
$H^{14}CO_3$
shells
$Ca^{14}CO_3$
humus $^{14}CO_2$
LAKE
OCEAN
groundwater table
ageing
$+ Ca^{12}CO_3 + H_2O \rightarrow H^{14}CO_3^- + H^{12}CO_3^-$

COSMIC BACKGROUND REDUCTION IN THE RADIOCARBON MEASUREMENTS BY LIQUID SCINTILLATION SPECTROMETRY AT THE UNDERGROUND LABORATORY OF GRAN SASSO

Wolfango Plastino[1] • Lauri Kaihola[2] • Paolo Bartolomei[3] • Francesco Bella[4]

ABSTRACT. Radiocarbon measurements by two 1220 Quantulus™ ultra low background liquid scintillation spectrometers were performed at the underground laboratory of Gran Sasso and the Radiocarbon Laboratory of E.N.E.A.-Bologna to study the efficiency and background variations related to measurement sites. The same configuration setup, i.e. the same center of gravity of the ^{14}C spectrum (SQP(I) = 410 ± 1) was obtained in both instruments. Many different background and modern standards with pure analytical benzene were used and spectra for 40 one-hour periods were obtained. The data indicates a background reduction of approximately 65% between the surface and underground laboratories, with no differences in the efficiency. Recording similar efficiencies in both spectrometers is probably due to fairly identical photomultiplier characteristics. The cosmic noise reduction observed at the laboratory of Gran Sasso makes it possible to perform high precision ^{14}C measurements and to extend for these idealized samples the present maximum dating limit from 58,000 BP to 62,000 BP (5 mL, 3 days counting).

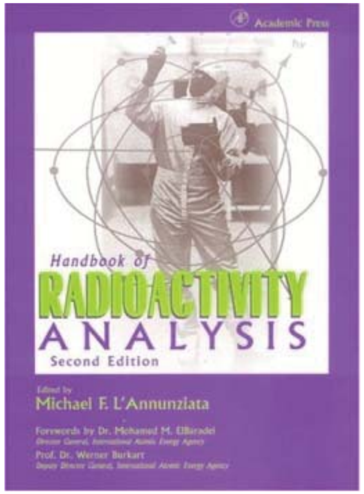

...the best result around the world

Sample	Count rate (cpm)	Count error (cpm)	Modern activity (dpm)	Modern activity error (dpm)	Eff (%)	FM	fM	T_{max} (BP)
L1A	0.278	0.022						
H1A	12.949	0.148	8.853	0.088	80.93	25,531.503	17	48,200
L1A	*0.059*	*0.010*						
H1A	*12.282*	*0.144*	*8.540*	*0.094*	*76.76*	*99,734.000*	*35*	*54,000*
L3A	0.398	0.026						
H3A	39.140	0.257	27.068	0.161	83.28	17,419.104	43	55,900
L3A	*0.150*	*0.016*						
H3A	*38.235*	*0.254*	*26.609*	*0.166*	*81.35*	*44,052.587*	*69*	*59,600*
L5A	0.655	0.033						
H5A	65.206	0.332	45.101	0.209	83.60	10,676.865	57	58,000
L5A	*0.235*	*0.020*						
H5A	*63.874*	*0.328*	*44.464*	*0.215*	*81.89*	*28,580.867*	*92*	*61,900*

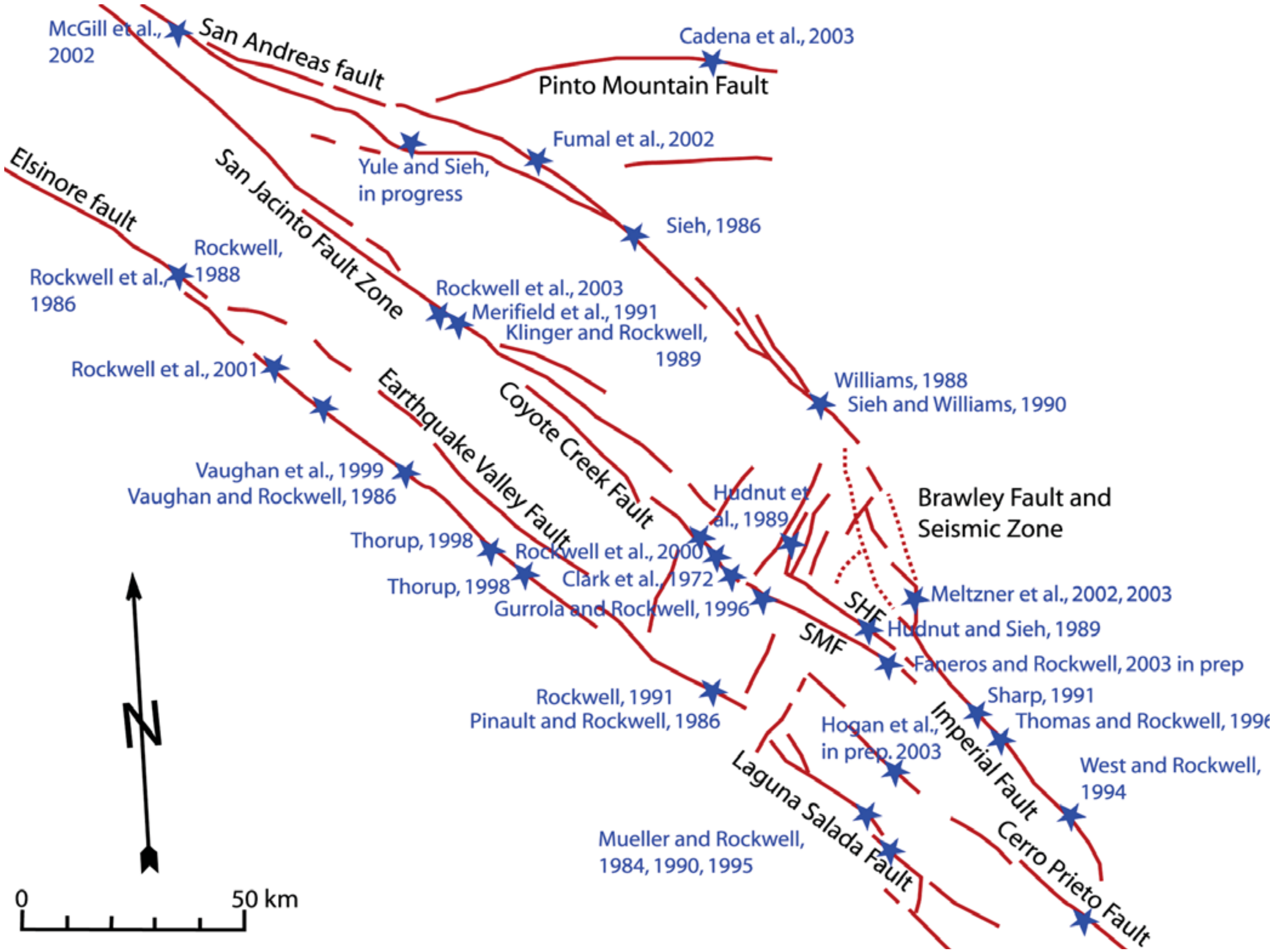

© Rockwell San Diego Univ.

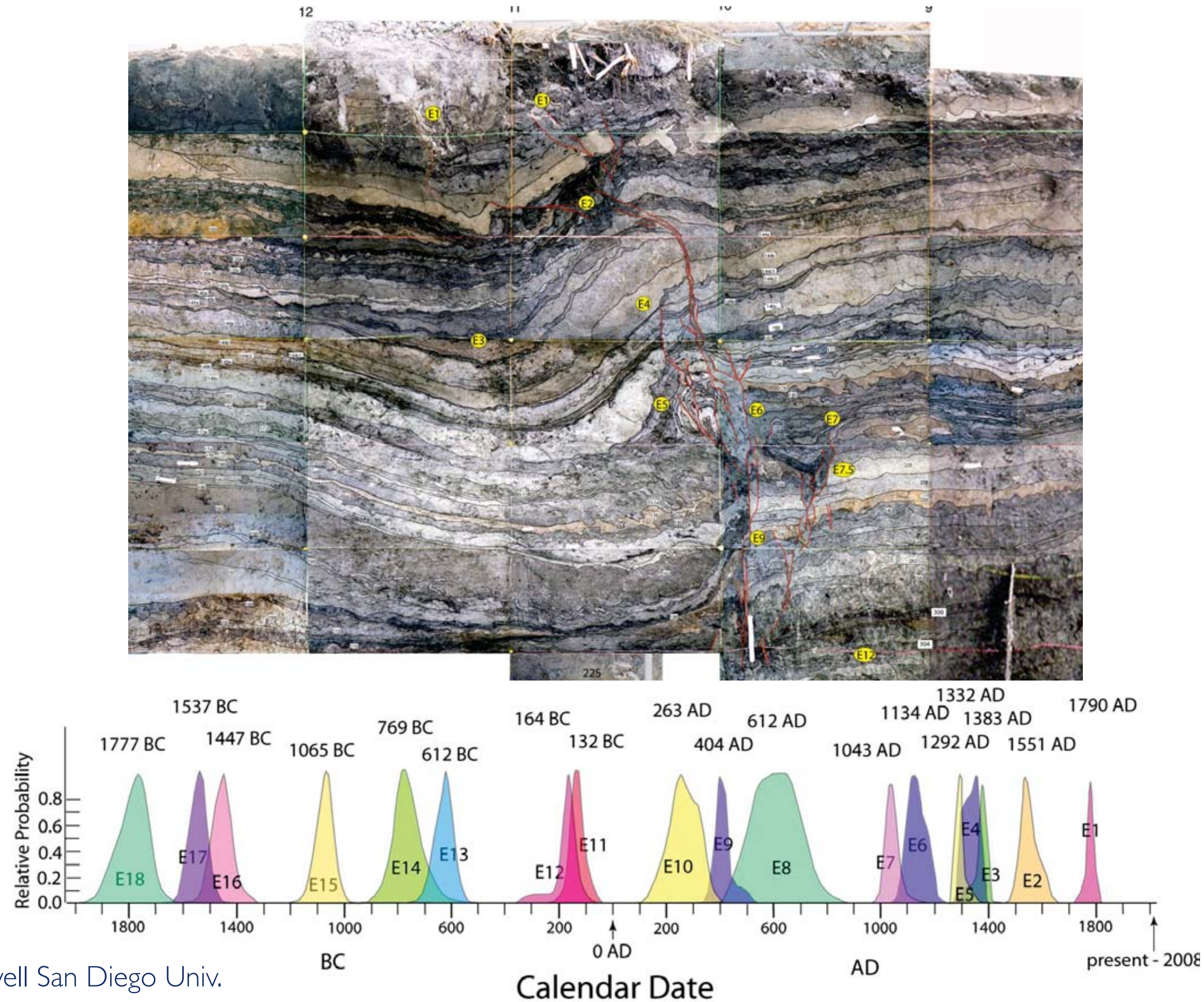

© Rockwell San Diego Univ.

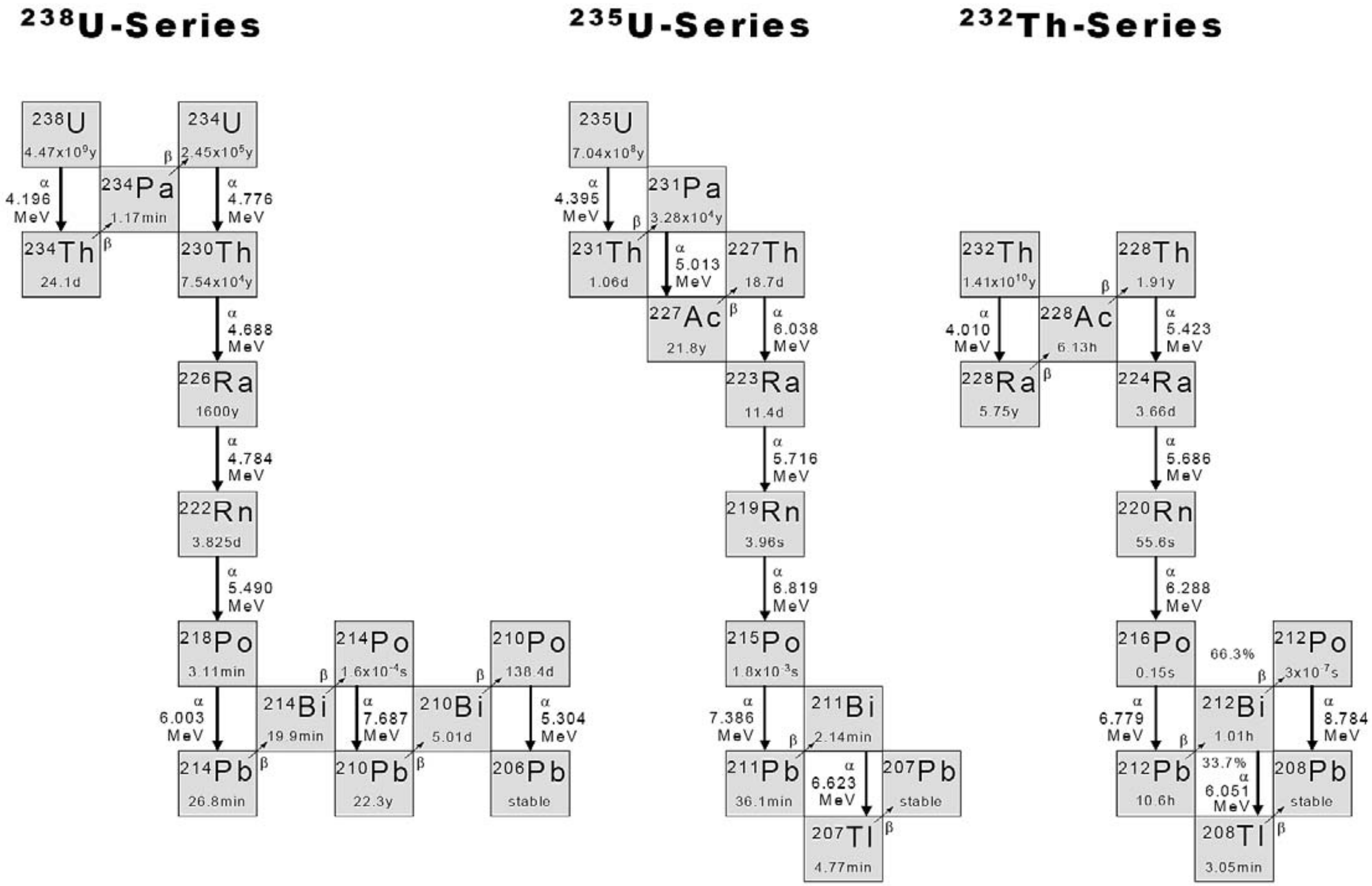
238U-Series
235U-Series
232Th-Series
238U 4.47x10^9y
234U 2.45x10^5y
234Pa 1.17min
234Th 24.1d
230Th 7.54x10^4y
226Ra 1600y
222Rn 3.825d
218Po 3.11min
214Bi 19.9min
214Po 1.6x10^-4s
214Pb 26.8min
210Pb 22.3y
210Bi 5.01d
210Po 138.4d
206Pb stable
α 4.196 MeV
α 4.776 MeV
α 4.688 MeV
α 4.784 MeV
α 5.490 MeV
α 6.003 MeV
α 7.687 MeV
α 5.304 MeV
β
235U 7.04x10^8y
231Pa 3.28x10^4y
231Th 1.06d
227Th 18.7d
227Ac 21.8y
223Ra 11.4d
219Rn 3.96s
215Po 1.8x10^-3s
211Bi 2.14min
211Pb 36.1min
207Pb stable
207Tl 4.77min
α 4.395 MeV
α 5.013 MeV
α 6.038 MeV
α 5.716 MeV
α 6.819 MeV
α 7.386 MeV
α 6.623 MeV
232Th 1.41x10^10y
228Th 1.91y
228Ac 6.13h
228Ra 5.75y
224Ra 3.66d
220Rn 55.6s
216Po 0.15s
212Po 3x10^-7s
212Bi 1.01h
212Pb 10.6h
208Pb stable
208Tl 3.05min
α 4.010 MeV
α 5.423 MeV
α 5.686 MeV
α 6.288 MeV
α 6.779 MeV
α 8.784 MeV
α 6.051 MeV
66.3%
33.7%

Alpha Decay

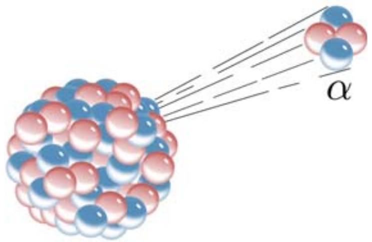

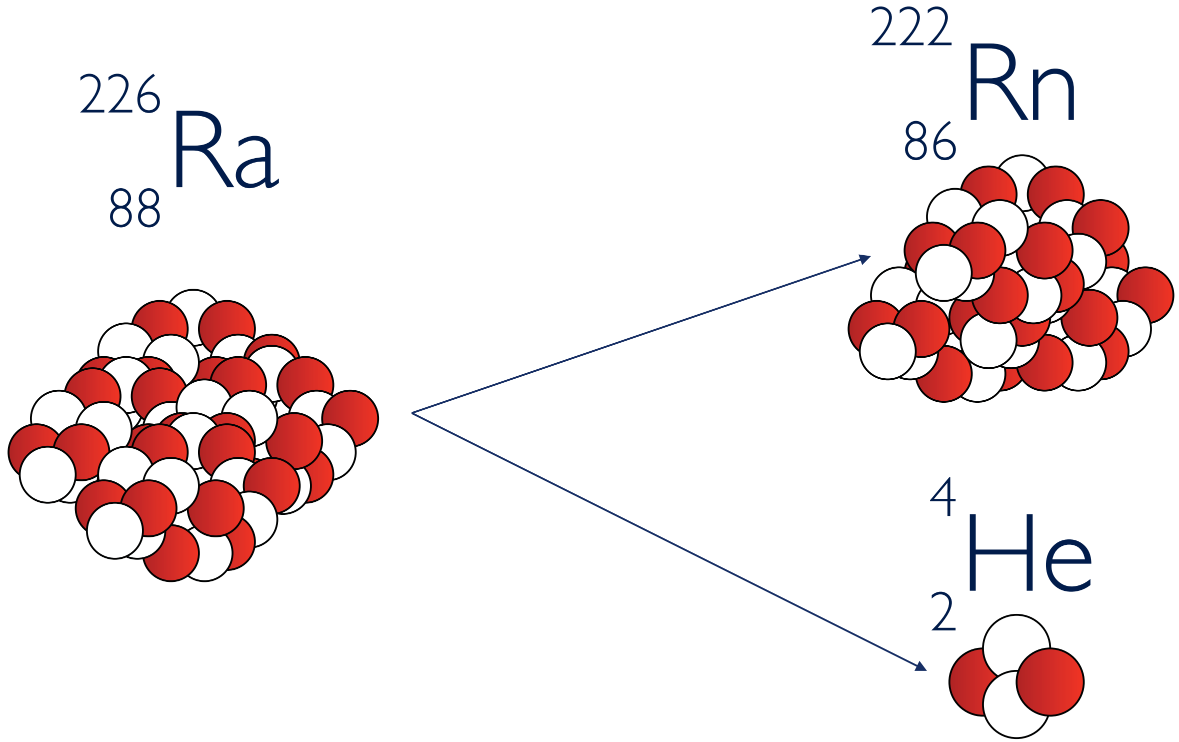

$$^{A}_{Z}X \longrightarrow \, ^{A-4}_{Z-2}Y + \, ^{4}_{2}He$$

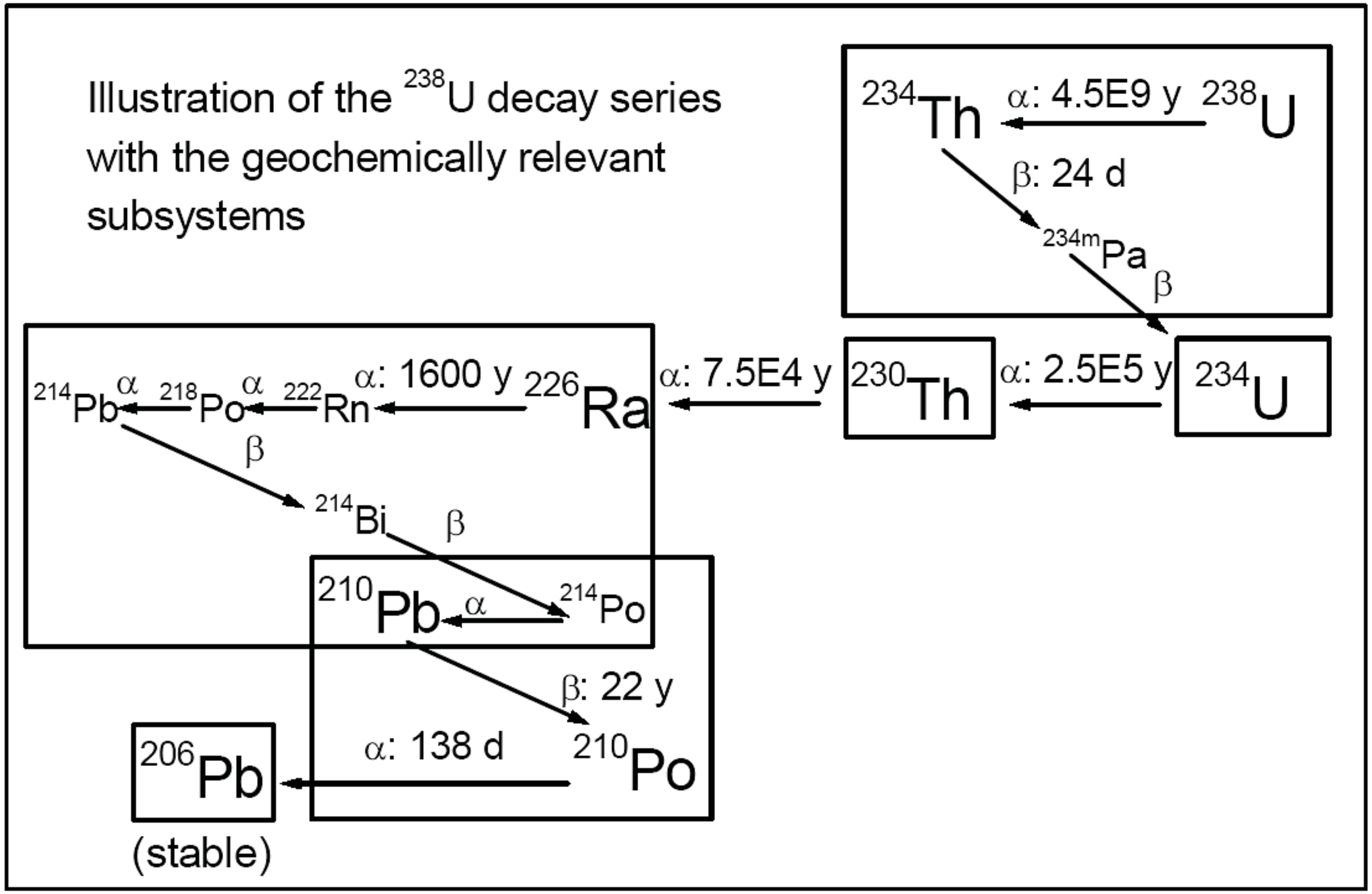
Illustration of the 238U decay series with the geochemically relevant subsystems
234Th
α: 4.5E9 y
238U
β: 24 d
234mPa
β
α: 7.5E4 y
230Th
α: 2.5E5 y
234U
214Pb
α
218Po
α
222Rn
α: 1600 y
226Ra
β
214Bi
β
210Pb
α
214Po
β: 22 y
α: 138 d
210Po
206Pb
(stable)

Natura non facit saltus

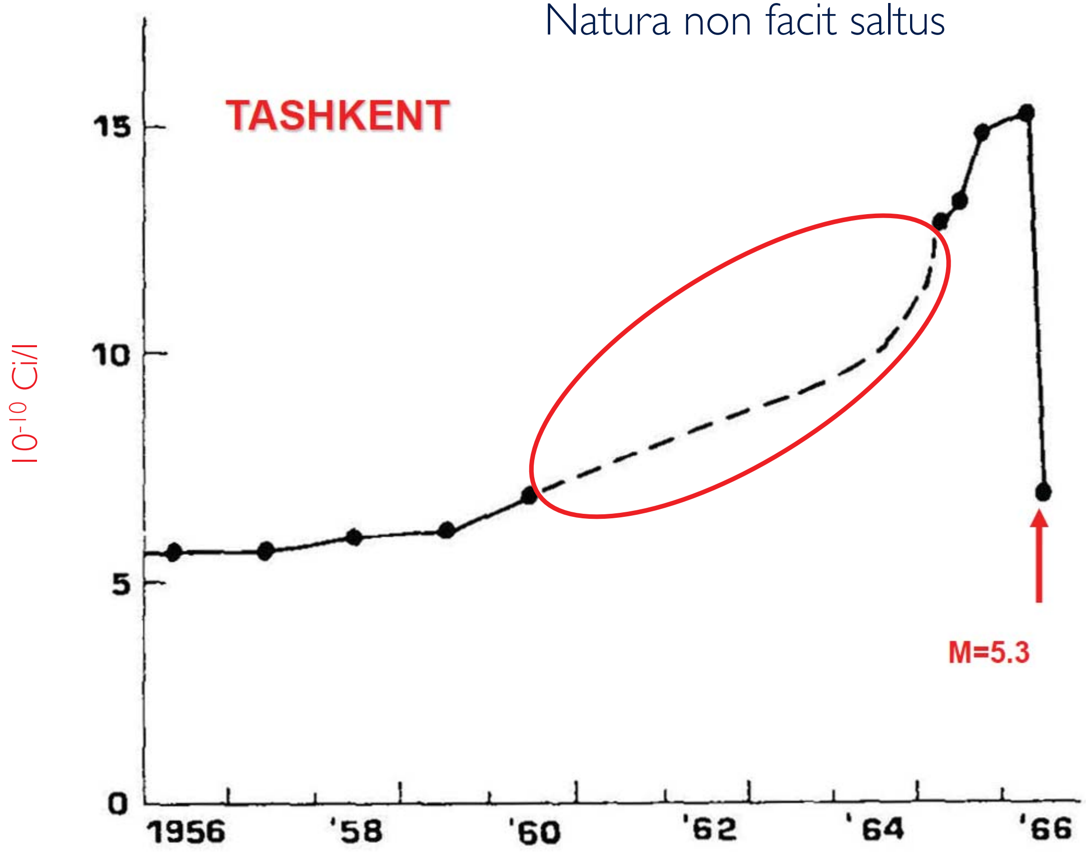

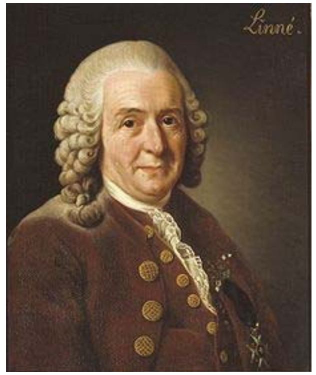

Ulomov, V.I., Mavashev, B.Z., 1967. A precursor of a strong tectonic earthquake. Doklady Akademii Sciences SSSR, Earth Sciences Sections 176, 9–11.

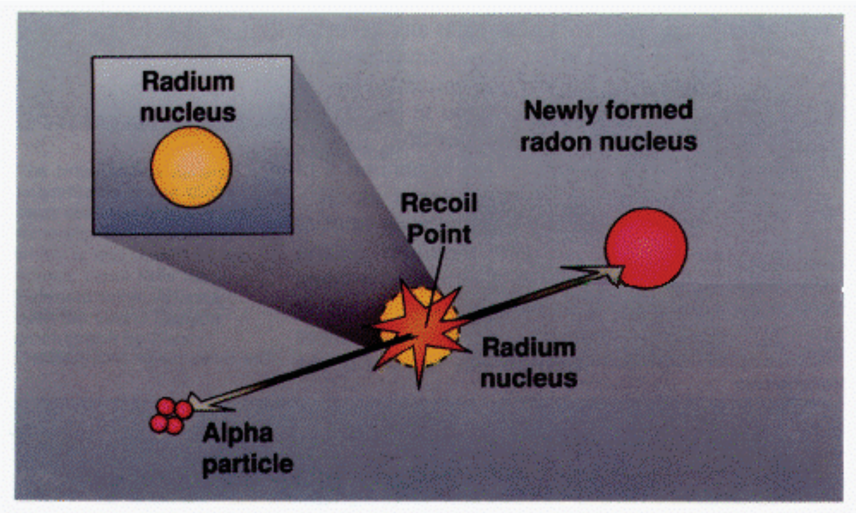

Radium decay involves the release of the excess energy which is shared between the α particle which forms (98.1%), and the new radon atom

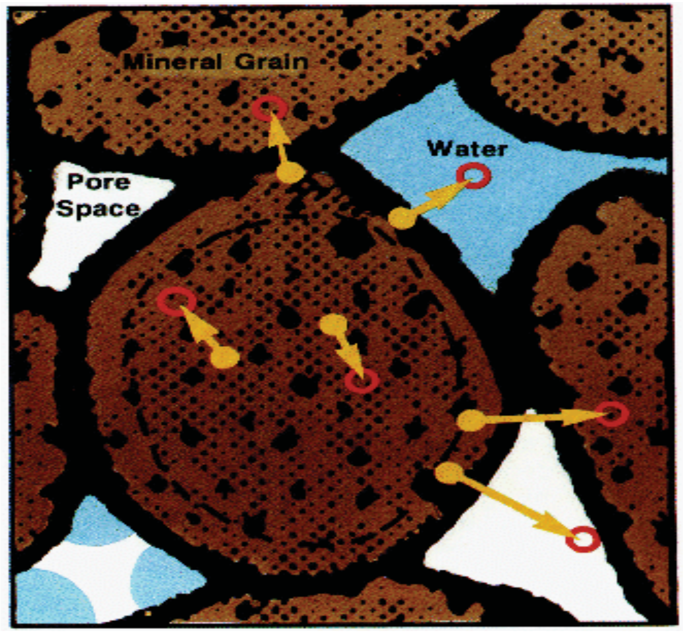

The emanating power of rocks is defined as the ratio between the amount of radon escaping from the solid matrix and that produced by radioactive decay

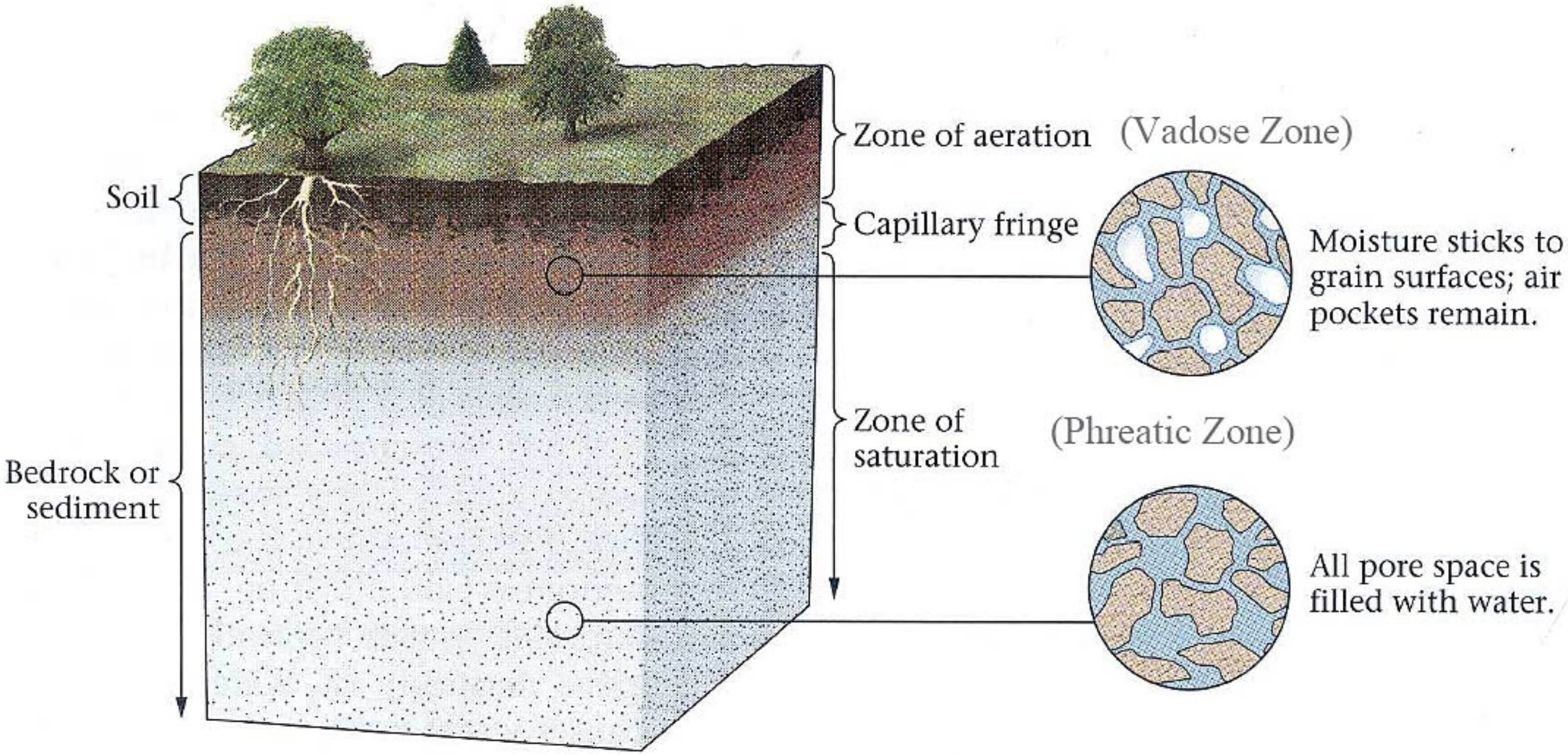
Zone of aeration
(Vadose Zone)
Soil
Capillary fringe
Moisture sticks to grain surfaces; air pockets remain.
Zone of saturation
(Phreatic Zone)
Bedrock or sediment
All pore space is filled with water.

Earth science

Radon and rock deformation

Evelyn Roeloffs

What happens when stress is applied to rocks in the Earth's crust so that the crust deforms? This is a question tackled by Trique *et al.* on page 137 of this issue[1]. They have used a natural laboratory in the French Alps — the Roselend reservoir — to monitor the geophysical signals that result from the greater or lesser pressure on the underlying crust exerted by the weight of water in the reservoir. This area is not itself prone to earthquakes. But the broader interest of this work is in what it may tell us about the events, induced by crustal deformation, that precede earthquakes.

The ability to predict earthquakes is of course highly desirable. But progress in this difficult and highly contentious science will depend on detecting and interpreting physical changes stemming from the processes of earthquake generation. Many possible precursors have been reported, but seismologists are sceptical of those that are not clearly linked to crustal deformation. This 'unproven' category includes the well-documented precursory decrease and increase of radon concentration before the 1978 Izu–Oshima earthquake in Japan[2] (Fig. 1), as well as the controversial assertion that deformation of crustal rocks.

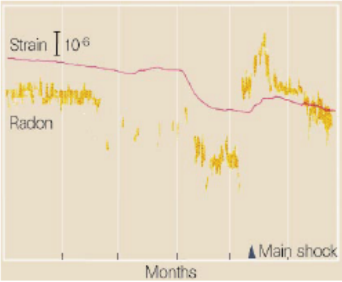

Figure 1 **The radon and strain data for the magnitude-7 Izu–Oshima earthquake[2,9] of 14 January 1978 show changes preceding the earthquake. But they do not match the model shown in Fig. 2; in particular, neither change is monotonic, and in both cases the pre-earthquake change exceeds that produced by the earthquake itself.**

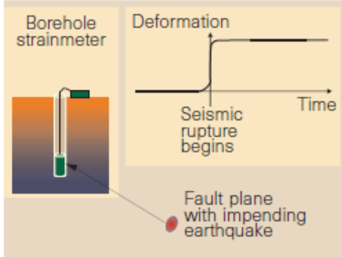

Figure 2 **Rock friction, which depends on slip rate and sliding-induced changes on a fault surface, implies that seismic slip should be preceded by accelerating aseismic slip near the hypocentre of an impending earthquake. Sufficient aseismic slip would produce near-surface deformation detectable by a borehole strainmeter. Compared with the strain step recorded at the time of the earthquake, the precursory strain signal would be in the same direction but of much smaller amplitude. A magnitude-5 earthquake, 10 km deep, produces maximum near-surface strain of about 10^{-7} at a site 5 km from its fault plane; strain increases 30-fold for each unit increase of magnitude, but falls off as the third power of distance from the source. Estimates of pre-seismic slip duration and amplitude range widely because frictional parameters of natural faults are poorly known.**

Seismologists expect earthquake precursors to take the form of transient crustal-strain signals from 'aseismic' fault slip near the earthquake's nucleation point (that is, fault slip that is too slow to radiate seismic waves) (Fig. 2). Numerical simulations show, however, that such signals would be exceedingly small[4]. Even the best existing instruments — borehole strainmeters with resolution exceeding a part per billion — would need to be within a few kilometres of the impending earthquake's epicentre to detect this aseismic strain. Although strain changes preceding two California earthquakes have been identified[5,6], they don't resemble the expected signals.

Proponents of earthquake prediction maintain that changes in radon emission, or in electrical or magnetic fields, represent a natural amplification of pre-earthquake deformation under special geological conditions. For example, the conductance by rock fractures of water or gas is proportional to the third power of the fracture's aperture[7]. Fluid flow past ions adsorbed on rock surfaces produces an electric field, termed a 'streaming potential', that varies with pressure gradient and permeability[8]. Fluid, gas or electromagnetic measurements might thus detect deformation indirectly, albeit at localized sites and with amplitudes related nonlinearly to strain.

Silver and Wakita[9] list many potential examples of such pre-earthquake 'strain indicators'. Unfortunately, these indicators are irreproducible: they can be detected only in certain locations, but in any one location earthquakes recur infrequently. What is needed is evidence that transient strain leads consistently, if not linearly or uniformly, to observable phenomena. The radon, electrical and ground-tilt measurements from Roselend lake constitute this kind of reproducible evidence.

The shallow crust's reaction to large changes in lake level may also illuminate the

...to be continued